Environmental flow provision: Implications for agricultural water and land-use at the global scale

Abstract

Human activity poses a severe threat to freshwater ecosystems. It has led to ecosystem degradation in the past and is likely to continue doing so if no appropriate protection mechanisms are implemented. One potential protection measure is the reallocation of water from human use to environmental purposes – also called environmental flows. Such reallocation may decrease irrigation water availability with possible adverse effects on agricultural production. With this analysis, we provide a first quantitative estimate of how the allocation of annual volumes of water for environmental flow protection (EFP) may influence the food production system at the global scale. The application of a spatially explicit global land and water-use allocation model (MAgPIE) allows us to explore the effect of EFP on agricultural water withdrawals as well as associated reactions in terms of land-use changes and agricultural intensification. Our results suggest that the implications of conserving annual volumes of water for EFP on the land-use system are moderate on an aggregate global level. Cropland expansion into unmanaged land due to increasing food demand until 2045 is by a factor 5 to 9 higher than cropland expansion induced by EFP. Global forest losses associated with EFP stay below 1% of current forest area. Production reallocation and associated land-use change hotspots suggest that local effects are of more concern than aggregate cropland expansion and deforestation.

Keywords

Environmental flows; water-use; land-use; land-water-nexus; sustainability; global; model

1 Introduction

Freshwater is indispensable for sustaining life on Earth and adequate freshwater availability is essential for human well-being (Oki, 2006). Direct human water abstraction involves water for irrigated crop production, energy production, industrial fabrication, and domestic purposes (Flörke et al., 2013). Additionally, humanity benefits from a variety of services provided by freshwater ecosystems. Those include the provision of fish, other food and fiber, water purification, erosion protection, biodiversity conservation and cultural and recreational benefits (Poff et al., 2010; UNESCO, 2009). The third World Water Development Report by the (UNESCO, 2009) highlights that the economic value of freshwater ecosystem services exceeds $600 million in Uganda alone and that 10% of undernourished people depend on freshwater ecosystem services across developing countries.

At the same time, it is widely recognized that human disturbance leads to degradation of freshwater ecosystems (Grafton et al., 2012; Hoff, 2009; Poff et al., 2010). It has been estimated that freshwater vertebrate populations have declined by 54 % globally and that 32 % of the world's amphibian species are threatened with extinction (Dudgeon et al., 2006). Increasing human water demand due to population growth and economic development is likely to put additional pressure on freshwater resources in the future (Vorosmarty et al., 2010). This has led to the call for water management strategies that explicitly recognize environmental water requirements (Falkenmark and Molden, 2008). Sustaining river ecosystems and associated livelihoods requires the provision of environmental flows (EFs) that assure sufficient quantity, quality and timing of stream-flow (Poff et al., 2010). However, focusing on a single conservation goal can lead to negative feedbacks on other ecosystems (Bennett et al., 2009; Seppelt et al., 2013). Therefore, environmental flow protection (EFP) cannot be pursued in isolation but has to be put into a broader context of sustainable use of natural resources (Gerten et al., 2013).

Freshwater use for irrigation accounts for around 70% of human water withdrawals (Rost et al., 2008) and plays an important role in global food production (Naylor, 1996). Since allocation of water resources for environmental purposes reduces available water for other uses (Falkenmark and Molden, 2008), EFP is likely to reduce water available for irrigation (Rosegrant et al., 2009; Strzepek and Boehlert, 2010). A reduction of irrigation potential may have adverse effects on food prices (de Fraiture and Wichelns, 2010) and the agricultural production required to provide sufficient amounts of food for a growing world population (Falkenmark et al., 2009; Rosegrant et al., 2009). Moreover, decreased land productivity due to irrigation water shortages may trigger cropland expansion (Lambin and Meyfroidt, 2011) at the expense of natural forests and other unmanaged land (Foley et al., 2011). Those land cover types are important for a variety of ecosystem services including biodiversity conservation (Barlow et al., 2007) and carbon sequestration (Onaindia et al., 2013).

It is therefore important to assess the feedback of EFP on land-use change in order to provide the knowledge needed to design sustainable water management strategies (Pahl-Wostl et al., 2013c).

While the design and implementation of EFP policies needs to be tailored to local conditions (Arthington et al., 2006), it is also necessary to adopt a global point of view in order to account for non-local drivers of water and land-use such as agricultural trade, population growth and economic development (Hoekstra, 2010; Hoff, 2009). Global investigations of the effects of EFP on agriculture are however lacking to date. Strzepek and Boehlert (2010) have studied the effects of providing annual volumes of water for EFP on current agricultural water availability. However, they do not investigate, what adaptation mechanisms in the agricultural system are to be expected and what consequences these reactions entail for global land-use change.

This article aims at providing a first quantitative estimate of how a reduction of water available for agriculture due to allocation of annual volumes of water for EFP may affect land-use change at the global scale. We compare scenarios including reservation of the annual water quantity needed for EFP to a business as usual scenario without EFP. Global land-use patterns, yield increases and agricultural water withdrawals under biophysical and socioeconomic constraints are simulated by the spatially explicit global agricultural land and water-use model MAgPIE (Model of Agricultural Production and its Impacts on the environment) (Lotze-Campen et al., 2008; Popp et al., 2010). This setup allows us to quantify the effect of conserving annual volumes of water for EFP on agricultural water withdrawals as well as associated reactions in terms of land-use change and agricultural intensification under different future socioeconomic conditions.

2 Methods

2.1 Model description MAgPIE

2.1.1 General model description

MAgPIE is a spatially explicit global land and water-use allocation model that simulates in 10 year time steps from 1995 to 2045 using recursive dynamic optimization (Lotze-Campen et al., 2008; Popp et al., 2010). The model's objective function is to fulfill demand for food, livestock and materials at minimum costs under biophysical and socio-economic constraints. Demand and socio-economic constraints are defined at the regional level (10 world regions, Figure A1). Biophysical constraints enter the model at grid cell level (0.5 x 0.5 degree longitude/latitude; 59199 grid cells). Due to computational constraints, grid-cells are aggregated to 1000 simulation units globally (Figure A2) based on similarity of biophysical conditions (Dietrich et al., 2013a). Demand scenarios are based on exogenous population, income and diet projections (Section 2.2.2). The production function takes land, water, yield information and monetary costs as inputs. MAgPIE endogenously determines cropland (rainfed and irrigated), forest and other natural vegetation patterns. Urban areas and pasture areas are assumed to be static over time and forest land is partly reserved for forestry activities and nature conservation (Section 2.2.2). Each land pool is initialized with historical patterns in 1995 (Krause et al., 2013). Crop yields (rainfed and irrigated) for 17 cropping activities , crop water demand and water availability are provided by the global vegetation and hydrology model LPJmL (Bondeau et al., 2007; Müller and Robertson, 2013). Yields are calibrated on a regional level to meet historical FAO cropland (FAOSTAT, 2013) in 1995.

Technological improvements have helped to increase yields in the past (Fischer and Edmeades, 2010). In MAgPIE, future yield increases from technological change (TC) are modelled endogenously. Landuse intensities (τ) for each region in 1995 are derived from historical data (Dietrich et al., 2012). Yields in MAgPIE scale linearly with τ and the model can invest into TC in order to increase τ (Dietrich et al., 2013b). The investment-yield ratio (IY; investments per unit of yield growth) is determined from historical data on total agricultural Research and Development spending (Pardey et al., 2006), agricultural infrastructure investments (transport, energy and water distribution, telecommunication and financial services; Narayanan et al., 2008) and yield data (FAOSTAT, 2013). A regression analysis is used to estimate the elasticity of IY with respect to τ (Equation 1).

$$IY(\tau) = (1900 \pm 400) \, * \tau^{\,2.4 \,\pm\, 0.9} \qquad (1)$$

Thus, yield improvements due to TC are more costly in intensive systems with high τ values where low-cost intensification options are already implemented. Factor requirement costs (capital, labour and chemicals, e.g. fertilizer) per hectare scale linearly with τ (Dietrich et al., 2013b).

Monetary costs for agricultural production comprise factor requirement costs, land conversion costs, transportation costs to the closest market, investment costs for irrigation infrastructure and investment costs for technological change. The cost minimization problem is solved through endogenous variation of rainfed and irrigated production patterns for 17 cropping activities (subject to regional trade constraints; Schmitz et al., 2012), land conversion (all at simulation unit level) and technological change (at regional level) (Lotze-Campen et al., 2010).

2.1.2 Water and irrigation representation

Water-use categories in MAgPIE include irrigation and livestock production, non-agricultural human water demand (domestic use, industrial use and use for electricity production) as well as environmental water requirements. Non-agricultural human water demand and environmental water requirements enter the model as exogenous scenarios (Section 2.2.2). Non-agricultural water demand is always fulfilled before agricultural water demand and thus effectively limits water availability for agriculture (similar to Elliott et al., 2013)). Livestock water demand per produced unit is derived from (FAOSTAT, 2005). Rainfed crop production is based on green water (precipitation infiltrated into the soil; Rost et al., 2008)) only. The model can endogenously decide to apply additional irrigation water from blue water resources (rivers, lakes, aquifers) in order to increase yields. The amount of irrigation water per hectare that has to be applied to a field is simulated by LPJmL as the soil water deficit below optimal plant growth (Rost et al., 2008) and corrected for losses from source to field of 36% based on Rohwer et al.

(2007). Thus, MAgPIE endogenously determines the extent of irrigated areas but does not allow for switching to supplementary irrigation if water becomes scarce. Yield increases through technological change are assumed to leave per hectare crop water demand unchanged, thus enhancing water productivity per ton (irrigation efficiency). This is in line with findings that yield increases and improved agronomic practices are essential for improving water productivity (Kijne et al., 2004; Molden et al., 2010; Rosegrant et al., 2009). Increased water productivity can be accomplished by e.g. : minimizing losses in the water distribution system; increasing the ratio of transpiration to evaporation on the field; increasing the ratio of harvested plant organ to total biomass production; increasing plant water-use efficiency by breeding and improved management of all inputs.

Water-use in MAgPIE is constrained by available blue water at simulation unit level. Available water is calculated on a 0.5 arc-degree grid using monthly hydrological inputs from LPJmL and subsequently aggregated to simulation unit level. For each river basin (Döll and Lehner, 2002), total annual runoff (precipitation that enters rivers, lakes and aquifers) in the basin constitutes the amount of water available in one year. The allocation of available water at basin level to the grid cells is based on the grid cells' monthly river discharge, i.e. the runoff accumulated along the river network. Each grid cell's fraction of total available basin water is calculated as the ratio of the grid cell's monthly discharge to the sum of the monthly discharge of all cells in the basin (Appendix equation A4). This procedure assures that water usage does not exceed available water at basin level and has also been used by Schewe et al. (2013).

It has however been highlighted that due to the seasonal distribution, not all blue water is accessible to humans (Postel et al., 1996). Quantifying this effect is difficult (Gerten et al., 2013) and annual water availability is often estimated in a rule of thumb manner by assuming a constant global availability fraction (Elliott et al., 2013) that differs across studies (Gerten et al., 2013). In this study, we use a process based estimate of the reduction of annual available water for irrigation due to seasonal variation. We assume that irrigation water can only be used by plants during their growing period. Therefore, we calculate the mean growing period over all crops for each grid cell and restrict available water for irrigation to the water available in this period. The following assumptions have been made for the mean growing period calculation:

- wintercrops in the northern hemisphere (sowing date later than June 30th and harvest date later than December 31st) are excluded assuming that no irrigation takes place during winter time in this region;

- for each grid cell, crops with yields below 10% of the world average yield are excluded. Such low yields indicate that the crop is not suitable for the location.

In grid cells where water storage facilities in terms of dams are present according to Biemans et al. (2011), the total annual blue water resource is available for irrigation. The resulting global water availability is 27000 km^3 per year.

2.1.3 Irrigation costs

Irrigated crop production is not only constrained by water availability but also requires irrigation infrastructure for water distribution and application. The initial pattern of area equipped for irrigation is taken from the AQUASTAT database (Siebert et al., 2007). MAgPIE can endogenously deploy additional irrigation infrastructure. Regional costs per hectare of expanding irrigation infrastructure in 1995 are derived from Worldbank data (Jones, 1995) and range from 1900 to 37200 US$ / ha (Appendix Table A1). Regional heterogeneity is largely driven by implementation difficulties such as funding shortage, procurement problems and construction quality (Jones, 1995). This is reflected by the comparatively higher costs in Africa and Latin America compared to Europe or Pacific Asia. Irrigation infrastructure costs are furthermore influenced by labor costs and the choice of irrigation technology (e.g. surface vs sprinkler irrigation; Rohwer et al., 2007). We assume that world regions will converge in the future with regard to economic, institutional and technological standards. Investment costs for irrigation infrastructure therefore converge linearly towards the European level of 5700 US$ / ha until 2050.

In order to conduct the presented analysis, we improved the model by including annual costs for irrigation (e.g. for water, fuel, labor and the maintenance of irrigation infrastructure). Unfortunately, there is no global dataset on irrigation costs available. Calzadilla et al. (2011) have however proposed an approach to extract the rent associated with the application of irrigation water (i.e. factor payments for irrigation water) from the GTAP land rent (i.e. payments for the factor land) (Narayanan et al., 2008). We largely follow the approach by Calzadilla et al. (2011) to determine the factor requirement costs for irrigation from the GTAP land rent. A detailed description of the calculations can be found in the Appendix (A2). The resulting annual irrigation costs (Appendix Table A2) range from 10 to 2000 US$ / ha for different crops and regions. 90% of the calculated costs are between 10 and 404 US$ / ha and only two values exceed 1000 US$ / ha (potato in the NAM and PAO). Case studies from the FAO report annual irrigation costs of 9.5 to 400 US$ / ha for different crops in African countries (Palanisami, 1997). Average annual irrigation costs for a selection of farms in the US range between 167 and 392 US$ / ha (Schaible and Aillery, 2013). Thus, our approximate calculation generally yields results that are comparable to observations from case studies.

2.2 Scenarios

We simulate global agricultural land and water use from 1995 to 2045 considering a total of eight scenarios that differ along two dimensions: environmental flow protection (four alternative futures) and socioeconomic development (two alternative futures). In order to limit the number of scenarios and to isolate the effects of EFP policies, climate change is not considered. All biophysical inputs are average LPJmL results for 1991-1999 throughout the simulation period. LPJmL is driven by climate data from the CRU 3.0 dataset (Mitchell and Jones, 2005). We furthermore test the sensitivity of our results with respect to technological change costs and irrigation costs.

2.2.1 Environmental flow protection scenarios

We compare scenarios where annual volumes of water are secured for environmental flow protection (EFP) from 2015 onwards to a baseline scenario without water allocation for EFP throughout the simulation period. The baseline assumption is based on findings that EF violation is a widespread global phenomenon. Hoekstra et al. (2012) have found that in 223 of 405 large river basins, EFs are violated at least one month per year. Furthermore it has been highlighted that current real-world water management rarely accounts for environmental water requirements (Arthington et al., 2010; Falkenmark and Molden, 2008).

For single river basins, EFs can be estimated with high confidence by applying holistic methods that combine hydrological, hydraulic and habitat simulation approaches (Pastor et al., 2013; Smakhtin and Eriyagama, 2008). Those can however not easily be scaled up since they rely on detailed site-specific data that is lacking at the global scale (Pastor et al., 2013). Therefore, global assessments like ours have to rely on approximate hydrological EF estimates based on modelled hydrological data. Over 200 EF estimation methods have been recorded (Arthington et al., 2006) and it has been highlighted that especially approximate hydrological methods are prone to large uncertainties (Poff et al., 2010; Smakhtin and Eriyagama, 2008). In order to account for this uncertainty, we consider three EFP scenarios with differing spatial EF patterns. For each EFP scenario, environmental water requirements are calculated from monthly hydrological data simulated by LPJmL on a 0.5 arc-degree grid. Subsequent aggregation to the 1000 simulation units used in this analysis and summation over all months results in annual volumes for EFP.

The first EFP scenario (Tennant) is based on an early study by Tennant (1976) who proposes to reserve 30% of available water for the environment in order to secure habitat for fishes, invertebrates and other wildlife and protect riparian vegetation from water stress. This threshold has subsequently been supported by a number of further studies (Hanasaki et al., 2008).

The second EFP scenario (Smakhtin) relies on research by (Smakhtin et al., 2004). They propose a combination of low-flow (LFR) and high-flow (HFR) requirements to sustain river ecosystems in a “fair” condition. The conservation goal is to limit species loss to very sensitive species and to limit intrusion by alien species. LFR correspond to the 90% quantile of annual flow (Q90), i.e. to the discharge that is exceeded in nine out of ten months. Variable rivers are characterized by low Q90 values. In such cases high-flow events are important for river channel maintenance, wetland flooding, and riparian vegetation. HFR of 20% of available water are therefore assigned to rivers with a low fraction of Q90 in total discharge. Rivers with a more stable flow regime receive a lower HFR. For calculation details see Appendix A3.

The third EFP scenario (Hanasaki) is constructed according to a study by Hanasaki et al. (2008). The method is based on case studies in semi-arid to arid regions. It considers deviations from natural hydrological conditions and estimates base flow requirements and perturbation requirements. Technically, the method classifies rivers into four categories based on monthly discharge (Table 1). EFs between 0% and 40% of available water are then assigned based on monthly discharge values and category specific thresholds (Table 1; Appendix A3).

River classification			**Monthly environmental flow requirement**	
Description	*Minimum monthly streamflow q_{min} (mm/month)*	*Maximum monthly streamflow q_{max} (mm/month)*	*Condition for monthly discharge q (mm/month)*	*Monthly flow requirement q_{env} (mm/month)*
Dry (dry throughout a year)	$q_{min} < 1$	$q_{max} < 10$	$0 \le q < 1$	$q_{env} = 0$
			$1 \le q$	$q_{env} = 0.1q$
Wet (wet throughout a year)	$10 \le q_{min}$	$100 \le q_{max}$		$q_{env} = 0.4q$
Stable (stable throughout a year)	$1 \le q_{min}$	$q_{max} < 100$		$q_{env} = 0.1q$
Variable (dramatic difference between rainy and dry season)	Other than above		$0 \le q < 1$	$q_{env} = 0$
			$1 \le q < 10$	$q_{env} = 0.1q$
			$10 \le q$	$q_{env} = 0.4q$

Table 1 Environmental flow requirements for the Hanasaki scenario. Table adopted from Hanasaki et al. (2008) The discharge unit (mm/month) corresponds to monthly discharge divided by the catchment area (see Appendix A.3 for details).

The three EF calculation methods result in significantly different EF patterns (Figure 1). The Tennant method is globally uniform. The Smakhtin method shows considerable spatial variation, estimating rather low EFs (20 – 30% of available water) in most regions of the world and high values up to 50% in North America, Europe, the Amazon region, Central Africa and Indonesia. The Hanasaki method results in lower EFs in North America, Europe and North Africa and higher values throughout the tropics and large parts of Asia. Despite spatial variations, the global average fraction of EFs over available water is similar for the three methods (Tennant: 30%, Smakhtin: 30%, Hanasaki: 29%).

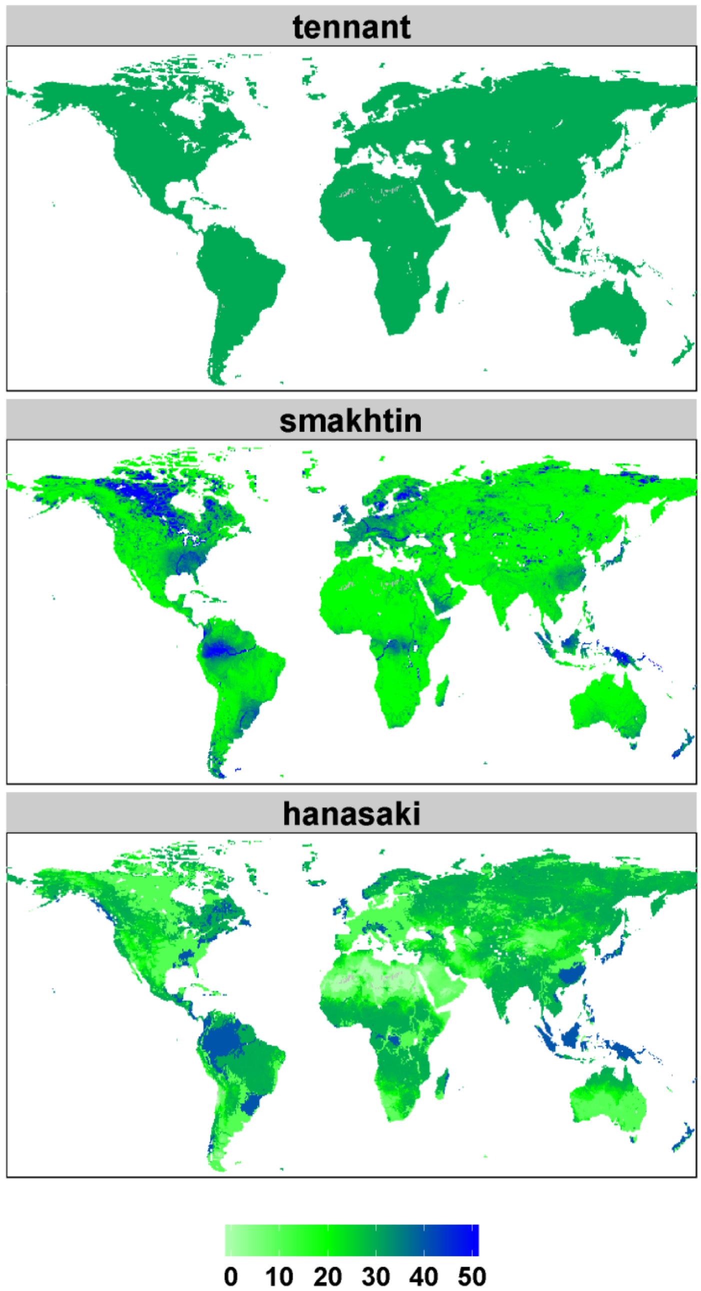

Figure 1 Environmental flow requirements over available water in per cent for the three EFP scenarios. Tennant method (top), Smakhtin method (middle) and Hanasaki method (bottom).

2.2.2 Socioeconomic scenarios

Since socioeconomic processes such as population growth, economic development and dietary preferences are key drivers of future land-use change (Popp et al., 2010), we conduct our analysis for two different socioeconomic scenarios. In order to span the plausible range of future conditions, we use two extreme cases from the SRES scenario family (Intergovernmental Panel on Climate Change and Working Group III, 2000). The A2 scenario is a high pressure scenario characterized by high population growth in developing regions (10.8 billion globally in 2045), self-reliance and regionally oriented economic development. In contrast, the B1 scenario depicts a world where global population growth slows down over the next decades reaching 8.6 billion in 2045. The emphasis of B1 is on global solutions to economic, social, and environmental problems. Within MAgPIE, these socioeconomic storylines are translated into scenarios for non-agricultural water demand (on simulation unit level), demand for agricultural products (on regional level), trade liberalization and forest protection as described below.

Spatially explicit non-agricultural human water demand for the domestic and industry sectors is obtained from the WaterGAP model (Alcamo et al., 2003; Flörke et al., 2013). Non-agricultural water demand is subject to structural and technological change and scales with population and economic activity according to the SRES storylines. Under the A2 scenario, global non-agricultural human water withdrawals more than triple until 2045 while they are almost constant under the B1 scenario (Figure 2).

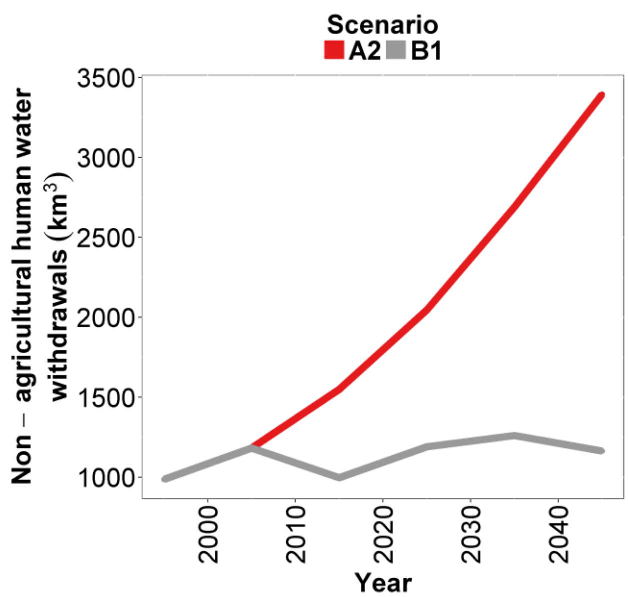

Figure 2 Global non-agricultural human water withdrawals including industrial production, domestic use and electricity production for the two socioeconomic scenarios. Data from WaterGAP (Alcamo et al., 2003; Flörke et al., 2013).

Global demand for agricultural products depends on population and food consumption per capita. Changes in regional food composition (e.g. livestock share) and per capita demand are driven by changes in per capita gross domestic product (Bodirsky et al., 2012). Food demand increases almost linearly from 2168 Mt dry matter in 1995 to 4745 Mt in 2045 under the A2 scenario (Appendix Figure A2). Under the B1 scenario, the increase is less pronounced and flattens out towards the middle of the century reaching 3892 Mt in 2045.

Agricultural trade between world regions in MAgPIE is fixed to historical trade patterns in 1995 and is liberalizing over time (Schmitz et al., 2012). The A2 scenario features little trade liberalization. In 2045, only 12% of total production can be allocated freely between the world regions based on competitive advantages. The remainder has to be produced regionally based on historical self-sufficiency rates and export shares. The B1 scenario allows for more interregional trade (35% free trade in 2045).

Forest protection comprises areas needed for wood production and natural conservation areas. Initial protection areas are derived from the FAO forest resource assessment (FAO, 2010) on a regional level and amount to ~1800 Mha globally. In A2, this area stays constant over time while in B1, forest protection areas increase linearly reaching ~2450 Mha globally in 2045.

2.2.3 Sensitivity analysis

In order to test the stability of our results with respect to economic assumptions, we conduct sensitivity analyses with respect to three crucial cost parameters.

Technological change costs: We vary the parameters of the cost function for technological change (Equation1) from their default values to the low and the high end of their uncertainty range.

Annual irrigation costs: We vary the annual costs for operation and maintenance of irrigation systems by ±30% around their default value.

Investment costs of irrigation infrastructure: In addition to the default setting of regionally converging costs, we consider a scenario with globally uniform investment costs (at the European level of 5700US$ / ha) and a scenario without convergence of regional costs to the European level.

3 Results

3.1 Development under business as usual scenarios

Before investigating the effects of environmental flow protection (EFP) by comparing our EFP scenarios to the baseline scenarios without EFP, this subsection highlights the water situation under a business as usual scenario. We concentrate on water scarcity projections and environmental flow (EF) violations. More detailed results regarding the general land- and water-use dynamics in the baseline scenarios can be found in the Appendix (Section B). These include comparisons with historical data for validation purposes.

3.1.1 Human water-use

In order to investigate human pressure on global renewable freshwater resources, we calculate the annual water withdrawal to availability ratio (WTA). For each socioeconomic scenario, total annual human water withdrawals in 2045 are divided by available water for the 1000 spatial simulation units (Figure 3). Many regions have a high WTA under both scenarios, especially in the USA, Mexico, the Middle East, parts of Africa, Southern Europe, India and Northern China. Under the A2 scenario, the WTA is higher than under B1, especially in the USA, Eastern Europe and the Middle East.

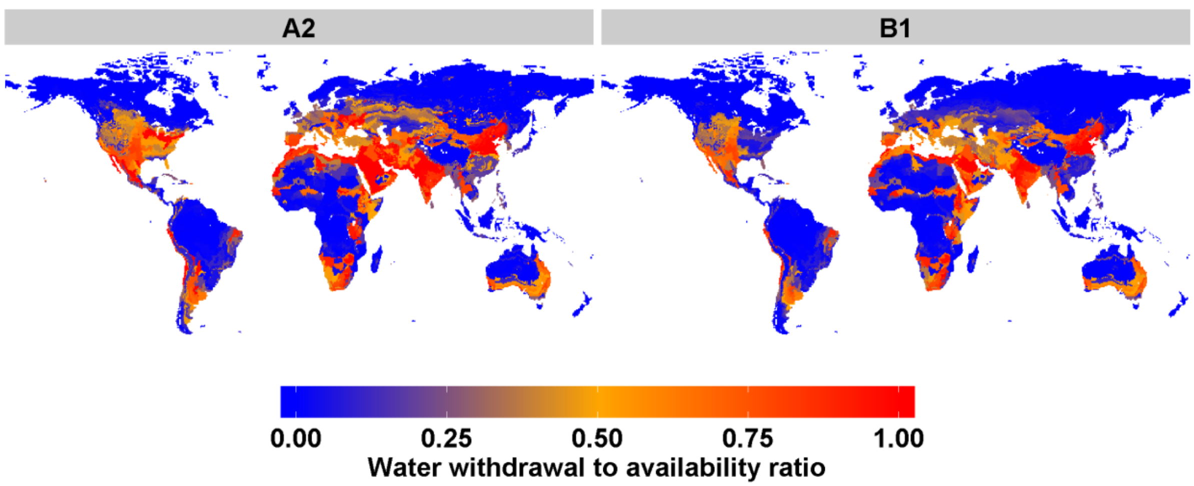

Figure 3 Human water withdrawal to water availability ratio under both socioeconomic scenarios without EFP in the year 2045. The index is zero if no water is used by humans and one if all available water is extracted.

3.1.2 Environmental flow violations

Where WTA values are high, annual human water withdrawals in the baseline scenario may tap into the annual volume of water required for EFP. We determine where the sum of baseline human water withdrawals in 2045 and estimated annual EF volumes (Section 2.2.1) exceeds available water for the three EF estimates considered in this analysis (Figure 4).

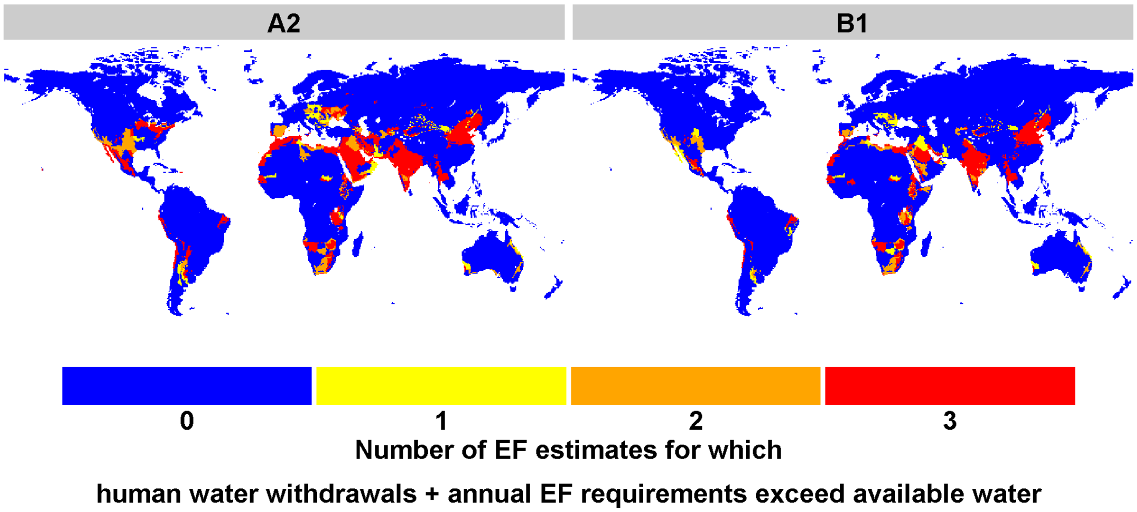

Figure 4 Violation of annual environmental flow requirements for the two socioeconomic scenarios in 2045 under baseline conditions. Colors indicate the number of EF estimates for which human water withdrawals in the baseline + annual EF requirements exceed available water.

Around 8% of global land surface (excluding Antarctica and Greenland) exhibits EF violation for both socioeconomic scenarios and all three EF estimates. These areas are responsible for ~10% of global agricultural production. The largest regions in this category are India, Northern China and the Middle East. Areas where at least one EF estimate under at least one socioeconomic scenario suggests EF violation cover 19 % of the global land surface and account for ~30% of global agricultural production. In A2, EF violation under all three EF estimates occurs on 12% of global land area while in B1 this is only the case for 8 % of land area. Regions where both socioeconomic scenarios exhibit EF violation under one or two EF estimates cover around 4 % of global land area.

3.2 Effects of environmental flow protection

This section concentrates on the differences between the EFP scenarios and the baseline scenarios.

3.2.1 Irrigated agriculture

All three EFP scenarios reduce agricultural water withdrawals (AWW) substantially under both socioeconomic scenarios (Figure 5, left). With increasing food demand and non-agricultural human water demand towards the middle of the century, the impact becomes more pronounced. By the mid of the century, AWW are reduced by 580 – 770 km^3 in the B1 scenario and 560 – 820 km^3 in the A2 scenario. Compared to simulated AWW for 1995 of 2840 km^3, this is a fraction of 20 – 27 % and 20 – 29 % respectively. Regional results show that under the A2 scenario, reductions of agricultural water withdrawals due to EFP are most pronounced in the Middle East and North Africa (Appendix, Figure C1).

These changes in AWW are driven by a reduction of irrigated areas (Figure 5, right). The pattern of changes across the scenarios is similar to AWW changes. Reductions of irrigated area in 2045 due to EFP amount to 48 – 61 Mha in the B1 and 54 – 82 Mha in the A2 scenario. This corresponds to 15 – 20 % (B1) and 17 – 26 % (A2) of modelled irrigated area in 1995 (312 Mha).

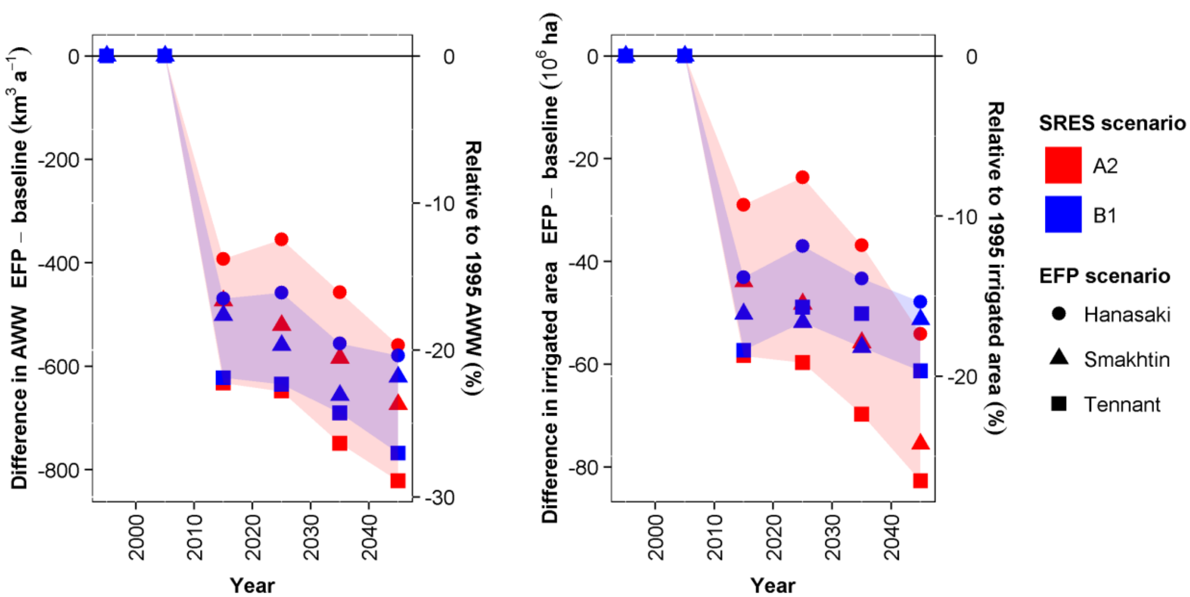

Figure 5 Changes in global agricultural water withdrawals (AWW, left) and global irrigated area (right) in the EFP scenarios with respect to the baseline for both socioeconomic scenarios. Colored points represent the three different EFP scenarios. Shaded areas span the full range of EFP impacts under the respective socioeconomic scenario.

3.2.2 Intensification versus cropland expansion into unmanaged land

Irrigated production accounts for around 40% of global agricultural production in our baseline scenarios. Since we assume that there is no demand-side reaction to the decrease in irrigated production capacity, the production losses due to EFP have to be compensated on the supply side. The two main mechanisms to increase agricultural production apart from increasing irrigation water inputs are cropland expansion and intensification, i.e. yield increases by better management and technological innovation (Lambin and Meyfroidt, 2011).

The reaction to EFP in terms of cropland changes shows strong variations and heavily depends on the socioeconomic as well as on the EFP scenario (Figure 6, left).
In the B1 scenario, cropland with EFP is higher than baseline cropland in all time steps under all three EFP scenarios. The maximum cropland increase with respect to the baseline is observed right after the implementation of the EFP policy in 2015 and amounts to 73 Mha. In 2045, the three EFP scenarios require 34 – 39 Mha additional cropland compared to the baseline. This corresponds to around 2 – 3% of simulated cropland in 1995 (1420 Mha).

In the A2 scenario, the picture is more diverse with strong variations between EFP scenarios especially in 2025. Between 2015 and 2025, cropland expands by 150 Mha in the baseline scenario. In the Hanasaki scenario, cropland only expands by 50 Mha. Shadow prices for land (Appendix Figure C2) and water (Appendix Figure C3) are higher for the Hanasaki scenario compared to the baseline, especially in Latin America, North America, Pacific Asia, and South Asia. This indicates that the water constraints in the Hanasaki scenario limit the availability of attractive production sites. Consequently, the cost-optimal solution is less cropland expansion and stronger intensification (Figure 6, right) for the Hanasaki scenario compared to the baseline without EFP. In 2045, projected cropland expansion due to EFP amounts to 2 – 45 Mha (0 – 3% of simulated 1995 cropland). Cropland expansion especially in the Middle East and North Africa is restricted by limited land availability (Appendix Figure C4).

Agricultural intensification, i.e. an increase of agricultural yields by technological change and better management as a reaction to EFP can be observed in all scenarios (Figure 6, right). Under the A2 scenario, global yield increases from technological change of around 4 – 6 % with respect to the baseline are required in 2045. Under the B1 scenario, required yield increases are lower, peaking at 4 % in 2035 and reaching around 2 – 3 % in 2045. Land-use intensities under baseline conditions are shown in the Appendix (Appendix, Figure B4). EFP furthermore leads to reallocation of production between regions, especially in the B1 scenario with lower trade barriers (Appendix, Figure C5).

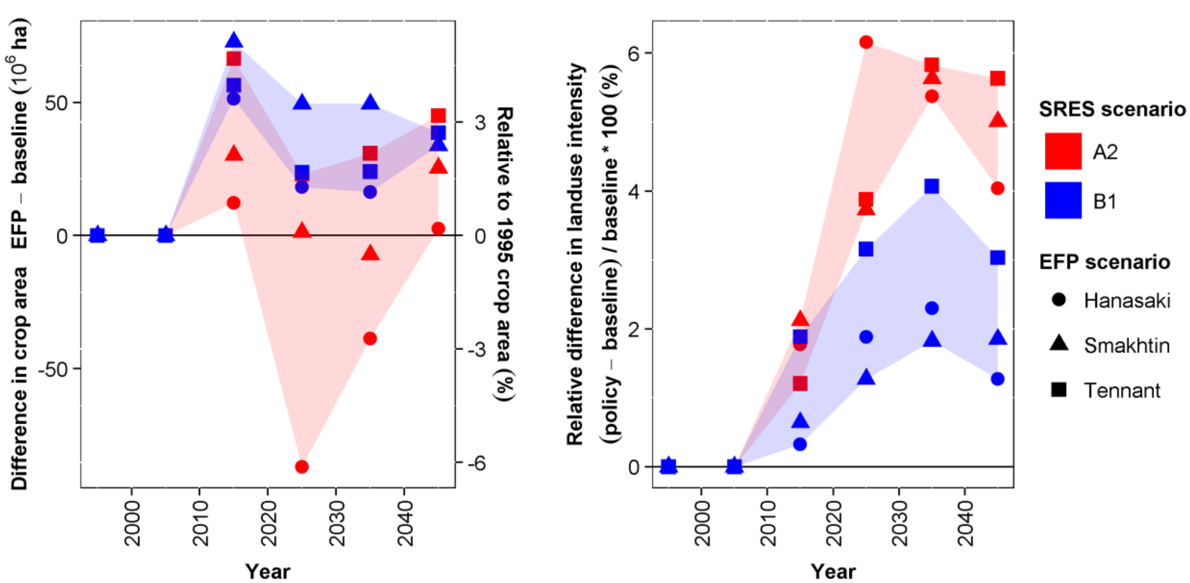

Figure 6 Changes in global crop area (left) and relative changes in land-use intensity (right) in the EFP scenarios with respect to the baseline for both socioeconomic scenarios. Colored points represent the three different EFP scenarios. Shaded areas span the full range of EFP impacts under the respective socioeconomic scenario.

Within MAgPIE, cropland expansion due to EFP can take place at the cost of unmanaged forests and other natural vegetation. In order to isolate the effects of EFP on natural forests, we determine the change in global forest area due to EFP (Figure 7). The general pattern of changes in forest area due to EFP is similar to the changes in crop area (Figure 6, left) because cropland expansion is the driver of deforestation.

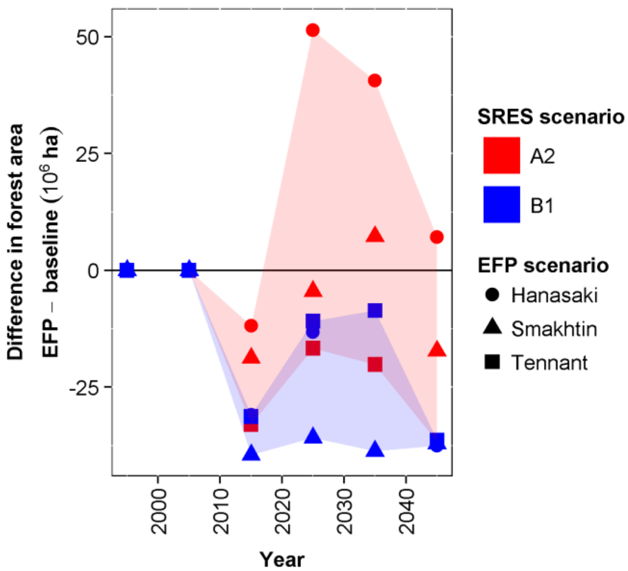

Figure 7 Changes in global forest area with EFP compared to the baseline for both socioeconomic scenarios. Colored points represent the three different EFP scenarios. Shaded areas span the full range of EFP impacts under the respective socioeconomic scenario.

Under the B1 scenario, losses of natural forests occur throughout the simulation period and under all EFP scenarios. The highest spread between different EFP scenarios can be observed in 2035 with deforestation of 9 – 39 Mha. In 2045, the model results for different EFP scenarios converge to ~37 Mha of forest lost. For the A2 scenario, differences between EFP scenarios are most pronounced in 2025 with changes in forest area of -17 to 51 Mha. Positive values (more forest area with EFP) are a result of strong baseline deforestation between 2015 and 2025 (100 Mha). In the Hanasaki scenario, only 40 Mha of forest are lost during that period. By the mid of the century, changes in forest area are 7 to -37 Mha. In the Hanasaki scenario, EFP even leads to less deforestation than under baseline conditions.

In order to investigate where the pressure on land ecosystems due to EFP is high, we determine where cropland area changes due to EFP under the three different EFP scenarios. A spatially explicit index ranging from 0 to 3 is derived, indicating how many EFP scenarios lead to cropland expansion into unmanaged land (Figure 8, top) and to cropland contraction (Figure 8, bottom).

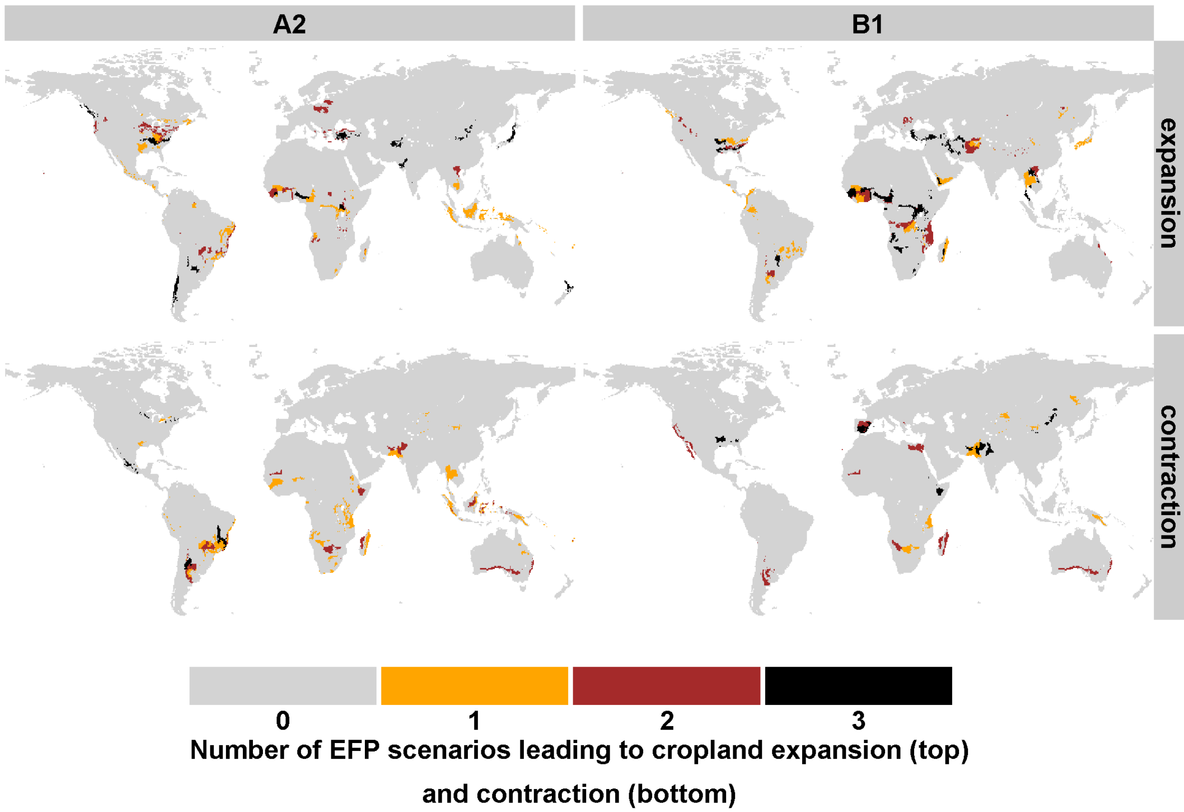

Figure 8 Locations where conserving annual volumes of water for EFP leads to cropland expansion into previously unmanaged land (top) and cropland contraction (bottom) for the two socioeconomic scenarios in 2045. Colors indicate the number of EFP scenarios that lead to cropland expansion / contraction at a given location. If changes in cropland extent stay below 1% of total land area, the location is marked as no change (0).

Under the A2 scenario, differences between EFP scenarios are high, indicated by the large areas where only one or two out of three EFP scenarios lead to cropland changes (Indonesia, USA, Africa and Brazil). Hotspots where cropland expansion is likely to occur are located in Argentina, Chile, the United States, Canada, Western and Central Africa, Northern China, Japan, Turkey, India and Afghanistan. Under the B1 scenario, land-use change hotspots are located in the USA, Western and Central Africa, the Middle East and South Asia.

3.2.3 Sensitivity analysis

Under the B1 scenario, the implications of EFP for global AWW and crop area in 2045 are in general robust against variations of technological change (TC) costs (Appendix Figure D1), annual costs for operation and maintenance of irrigation systems (Appendix Figure D2), and investment costs for irrigation infrastructure (Appendix Figure D3). Under the A2 scenario, high TC costs can lead to more cropland expansion due to EFP (up to 80 Mha in 2045) while low TC costs limit crop area expansion due to EFP in 2045 to 30 Mha. High annual irrigation costs increase cropland expansion due to EFP in A2 (up to 107 Mha in 2045) and decrease the EFP implications for crop area in B1 (below 30 Mha in 2045). Changes in irrigation infrastructure investment costs can lead to reduced crop area requirements with EFP compared to the baseline (up to 90 Mha in 2045).

4. Discussion

The presented study investigates how conserving annual volumes of water for EFP may affect global agricultural water-use and land-use dynamics under two different socioeconomic scenarios. Our modelling approach allows us to simulate spatially explicit global reactions of the land-use system to EFP without exogenously prescribing production patterns, irrigation patterns, trade flows or yield increases. This endogenous treatment of many key agricultural variables in a cost optimization framework is important in order to capture the linkages and cross dependencies in the land and water-use sector. Projected global AWW, irrigated area, cropland and land-use intensity under baseline conditions are consistent with historical data around the year 2000 (Appendix B).

4.1 Development under business as usual scenarios

Human pressure on water resources is projected to be strong under both socioeconomic scenarios indicated by high WTA values. Under the pessimistic A2 scenario featuring high population growth and little global cooperation, the fraction of global land area (excluding Antarctica and Greenland) with a WTA > 0.4 is 28%. This is in line with results from Alcamo et al. (2007) who estimated that in the 2050s, 26 to 28 % of total land area show a WTA higher than 0.4 for A2 depending on future climatic conditions. Our spatial patterns of WTA are similar in Latin America, Africa, the Middle East and Europe while we estimate higher WTAs in the east of the USA, Australia and China. One methodological difference is that Alcamo et al. assume constant irrigated area while we allow for expansion of irrigated agriculture. Therefore, agricultural water withdrawals are significantly higher in our analysis (3815 km^3 in 2045 for A2) compared to their projection of 2282 km^3 in 2055 leading to higher WTA values. Those higher WTA values are mostly concentrated in areas where Alcamo et al. (2007) also estimate WTAs >0.4 except for the differences mentioned above. An analysis by Shen et al. (2008) estimates agricultural water withdrawals of 4691 km^3 in 2055 under the A2 scenario which is higher than our estimate because the study assumes constant irrigation per capita and neglects water availability constraints. In the B1 scenario with low population growth and low trade restrictions, 22 % of the total land area have a WTA higher than 0.4. Lower WTAs compared to A2 are mainly due to lower non-agricultural human water withdrawals in B1 since AWW are similar for the two scenarios at the global level. Whether human water withdrawals are expected to tap into the water volumes needed for EFP does not only depend on the amount of water withdrawn but also on the underlying EF estimate. We estimate that the dependence of EF volume violations on socioeconomic drivers and EF estimates is equally pronounced.

4.2 Effects of environmental flow protection

4.2.1 Irrigated agriculture

Our results suggest that conserving annual volumes of water for EFP may substantially reduce the potential for irrigated agriculture to contribute to global food production by reducing AWW and irrigated area. This is in line with findings that environmental water requirements are the biggest threat to AWW compared to non-agricultural human water-use and climate change effects (Strzepek and Boehlert, 2010). In our results, reductions of AWW and irrigated area are sensitive to the EFP scenario but are similar for the socioeconomic scenarios. The spread between EFP scenarios is lower in B1, where more liberalized agricultural trade allows for compensating spatial differences in EF patterns between EFP scenarios.

4.2.2 Intensification versus cropland expansion

In our scenarios, the agricultural system reacts to EFP through intensification and cropland expansion. Reductions of agricultural water withdrawals due to EFP are most pronounced in the Middle East and North Africa, a region where no suitable land for cropland expansion is available. Latin America on the other hand, the region with the largest available land pool, is not strongly affected by EFP. Consequently, intensification is the main reaction to EFP under the A2 scenario with high population growth and strong trade restrictions. Under the B1 scenario, more liberalized trade allows for more reallocation of production to regions with abundant land resources (Africa and North America). Therefore, intensification due to EFP is less pronounced and there is a clearer trend towards cropland expansion for all EFP scenarios. Moreover, production reallocation under the B1 scenario reduces the spread of cropland expansion between EFP scenarios compared to A2. A rough calculation reveals the reason for the moderate feedback of conserving annual water volumes for EFP on crop area: irrigated agriculture accounts for around 40 % of total production in our scenarios, comparable to the 30 – 40 % reported by Rost et al. (2008). Reductions in irrigated area of ~20% therefore lead to global production losses of ~8% assuming homogenous yields. A major part of these production losses is then compensated by production reallocation and yield increases on current cropland.

4.2.3 Implications for forests and other unmanaged land

In our scenarios, cropland expansion due to allocation of annual water volumes for EFP can reduce global unmanaged natural land by up to 45 Mha by 2045. Around 80% of the loss of unmanaged land can be attributed to natural forests that mostly belong – according to our definition – to large intact forest landscapes (Krause et al., 2013) and represent valuable undisturbed ecosystems. The decline of land ecosystems could lead to biodiversity loss, carbon emissions and could adversely affect water regulation (Onaindia et al., 2013).

How do the benefits associated with conserving annual volumes of water for EFP (including the provision of food and fiber, water purification, biodiversity conservation, and erosion protection; Poff et al., 2010) compare to the detriments of losing 45 Mha of natural land ecosystems? Answering this question would require a detailed analysis of the quality and quantity of affected ecosystem services, would inevitably involve value judgments (Ford et al., 2009), and is therefore beyond the scope of this analysis. We can however analyze the additional challenges for sustainable land management strategies due to annual water allocation for EFP. To this end, we set the consequences of our EFP scenarios into the context of the general pressure on land ecosystems due to population growth and economic development under baseline conditions.

In our scenarios, global cropland expansion due to EFP by 2045 stays below 3% of the 1995 value. Expansion due to population and income growth under baseline conditions until 2045 is by a factor 5 to 9 higher (229 Mha in B1 and 413 Mha in A2). A recent agricultural model intercomparison used an ensemble of models to project cropland development under an SSP2 (IIASA, 2013) middle of the road scenario (Schmitz et al., 2014). Projected cropland expansion until 2050 for the ensemble mean without climate change is around 200 Mha, a factor 4 higher than our estimated impact of securing annual volumes of water for EFP. In our scenarios, long term deforestation associated with EFP corresponds to approximately 1 % of current global forest area (FAOSTAT, 2013) and twice the amount of forest lost annually in the period 2000-2012 of around 19 Mha (Hansen et al., 2013). The Hanasaki EFP scenario even leads to reduced deforestation compared to the baseline in A2.

Even though there is no major feedback of securing annual volumes of water for EFP on land-use change at an aggregate global level, local land-use change can impair the livelihood and wellbeing of people. Indigenous people and the rural poor are especially dependent on natural and wild resources (Naughton-Treves et al., 2005) that are threatened by land-use change. Environmental damages of local land-use change include biodiversity loss, soil erosion and changes in the water cycle (Klink and Machado, 2005). Due to the rather coarse resolution of 1000 spatial units, our modelling approach is not suited to investigate detailed local effects. Still, important insights can be gained from the patterns of cropland expansion hotspots due to EFP. Cropland expansion happens on 10% of global land area under at least one EFP scenario and at least one socioeconomic scenario. Less than 1% of global land area is affected by cropland expansion under all considered scenarios. This indicates that the pattern of land-use changes associated with EFP is highly dependent on the EFP scenario. Comparing the patterns of cropland expansion in the EFP scenarios to EF violation patterns under baseline conditions shows that there is little overlap between regions, where EF violations occur and where EFP leads to land-use changes. For both socioeconomic scenarios, around 90% of the area affected by cropland expansion under at least one EFP scenario is located in regions where no EF violations are observed in the baseline.

4.2.4 Implications of different environmental flow volume targets

Our three EFP scenarios differ in their impact on land-use change and deforestation because the spatial distribution of the EF volume targets is different. The globally uniform Tennant scenario has the strongest impact on global irrigated agriculture, land-use change, agricultural intensification, and deforestation. This indicates that spatial variation of EFs in the other two scenarios can be exploited by reallocating production in order to tap new water resources. This is also reflected in the strong dependence of spatially explicit land-use change patterns on the EFP scenario. The Hanasaki scenario has the least impact on land-use change and forest area at the global scale. Thus, from a global land-management perspective, the Hanasaki EF volume estimate is the best choice of the three considered methods.

The question, which of the three methods is most suitable concerning freshwater ecosystem protection, is more complex. There is a general agreement that freshwater ecosystem protection requires environmental flows that mimic natural conditions including the magnitude, timing, and frequency of flow events (Arthington et al., 2006). In this analysis, we concentrate on annual volumes of water for EFP and do not consider the timing within a year (see Section 4.3). However, the considered methods to estimate annual EF volumes differ in their accounting of flow variability and river-specific characteristics. The Tennant method does not consider intra-annual flow distribution. The Smakhtin method takes into account intra-annual flow variation to estimate low and high flow components of EFs. The Hanasaki method uses the most detailed rules (4 river categories, EF volume targets depending on monthly hydrological conditions) to estimate annual EF volumes. This suggests that the annual EF volumes of the Hansaki method are most appropriate for freshwater ecosystem protection, followed by the Smakhtin estimate and the Tennant estimate. However, a recent review of five global EF estimates involving a comparison to more detailed holistic EF estimates for 11 local case studies (Pastor et al., 2013) found that the Smakhtin and the Tennant method perform similar (R^2_{adj} = 0.86 and 0.88 respectively). The Hanasaki method was not tested. Thus, different detail of allocation mechanisms can lead to comparable results and it is likely that all three methods provide good estimates for some rivers and fail to do so for others.

In this analysis, we investigate the implications of global EFP regimes. While there is an increasing intervention of international law in water issues, water management in reality happens on local or country scale (Gupta et al., 2013). Our results indicate that securing annual volumes of water for EFP can lead to comparative disadvantages for food production. Local management authorities may therefore decide to implement EFs of low rigor or may not consider EFP at all. Fragmented EFP can lead to leakage of water stress due to production reallocation, i.e. to aggravation of water stress in regions without EFP. A fragmented EFP regime would likely put less pressure on global land-use and agriculture than a global EFP regime because more water would still be available for irrigation. Local production patterns might however change considerably.

4.3 Assumptions and limitations

Within our EFP scenarios, annual volumes of water are reserved for sustaining freshwater ecosystems. In reality, the functioning of such ecosystems depends on a variety of additional factors including water quality, the timing of stream flow within a year (Poff et al., 2010) and riparian land-use (Arthington et al., 2010). Thus, our EFP scenarios depict a world where a necessary step towards freshwater ecosystem protection is taken (managing water quantities) but where ecosystems may still face degradation due to factors that are not considered here. A comprehensive EFP policy that includes flow-timing and water quality aspects would likely increase the impact of EFP on agriculture.

EF requirements are highly dependent on the characteristics of individual river ecosystems and a thorough EF estimation requires site-specific data and a combination of hydrological, hydraulic and habitat simulation approaches (Pastor et al., 2013; Smakhtin and Eriyagama, 2008) that are not available at the global scale. The approximate global EF estimation methods that are applied here are therefore prone to large uncertainties (Poff et al., 2010; Smakhtin and Eriyagama, 2008). The three EFP scenarios in this analysis rely on different EF estimation methods in order to account for this uncertainty.

EFP can have many consequences across the Water –Energy–Food nexus including increasing prices for food and energy that influence equity and social stability (Ringler et al., 2013). Economic and social consequences of EFP depend on a variety of factors that are not considered in our analysis, e.g. market access, income distribution, and social welfare systems. Our study is therefore limited to the environmental tradeoff between water and land. Within our modelling framework, non-agricultural water demand does not react to EFP so that the water requirements for EFP have to be met at the expense of AWW. The justification of this assumption is the comparatively higher value of water in domestic and industrial sectors (Strzepek and Boehlert, 2010) and the high share of AWW in total human water-use.

Not all withdrawn water is consumptively used. Especially in non-agricultural sectors, the major part of withdrawn water returns to the river system and is available for downstream use after proper wastewater treatment (Flörke et al., 2013). Taking those return flows into account would require tracking water along the river network during the optimization, which is not feasible in our modelling framework due to computational limitations. This is a common issue of global water assessments (e.g. Alcamo et al., 2007; Chaturvedi et al., 2013; Sauer et al., 2010; Smakhtin et al., 2004; Strzepek and Boehlert, 2010) and it remains an open task to include a full river routing routine into global optimization approaches. We therefore cannot consider upstream-downstream interactions but we assure that water withdrawals on basin level do not exceed available water and that EF volumes are met in each simulation unit.

Our results are conditional on the underlying optimization structure and model parameterization. Validation against historical data demonstrates that the default parameterization of the MAgPIE model can reproduce key characteristics of the real system. Sensitivity with respect to future socioeconomic conditions is addressed by choosing two SRES scenarios. The sensitivity analysis with respect to technological change (TC) costs suggests that the potential to increase yields and irrigation efficiencies via TC is important for mitigating impacts of EFP on land-use dynamics. Further sensitivity analysis shows that model results are more sensitive to annual costs for irrigation than to investment costs for irrigation infrastructure. The balance between cropland expansion and intensification depends on the availability of suitable land. We do not consider dynamics of urban areas since they only account for ~1% of global land-area (Erb et al., 2007). The assumption of constant pasture areas is made because the extent of pasture areas only changed by around 27 Mha (<1%) in the period 1989 – 2009 (FAOSTAT, 2013) and future projections of pasture dynamics do not show a clear trend towards expansion or contraction (Schmitz et al., 2014; Smith et al., 2010). We do not explicitly model forest management in the current model version and keep forest areas needed for wood production and nature conservation static over time (around 43% of global forest area in 1995). It is not clear, how forest dynamics will affect future land availability since a wide range of plausible projections of future wood demand exist and future wood harvest yields are uncertain (Smeets and Faaij, 2007). Finally, it has been shown that dietary shifts and waste reductions can decrease the pressure on the agricultural system (Godfray et al., 2010; Popp et al., 2010; Smith et al., 2013). Allowing for such adaptation measures would likely decrease the impact of EFP on land-use change compared to our setup with exogenous food and material demand.

5. Conclusions

Today, we see an alarming decline of aquatic biodiversity (Pahl-Wostl et al., 2013b) and a lack of appropriate responses in terms of the implementation of sustainable water management policies (Pahl-Wostl et al., 2013a). This has led to the proposition of a scientific agenda concentrating on the generation of robust knowledge about cross-sectoral implications of water management strategies to support the transition towards a sustainable water future (Pahl-Wostl et al., 2013c). In this article, we estimate how global allocation of annual volumes of water for EFP may affect agricultural water-use and land-use change at the global scale until the mid of the century. While our study focuses exclusively on the reservation of annual water quantities, comprehensive EFP policies should also target water quality and the intra-annual timing of flows. Further research is therefore needed in order to incorporate those aspects into global analyses of the effects of EFP on land-use and agricultural water-use.

It has been shown recently that the amount of water available for human use strongly depends on the definition of environmental water requirements (Gerten et al., 2013). Our results show that the feedback of EFP policies on the land-use system also depends on the underlying protection scenario - in terms of absolute numbers as well as with regard to the spatial distribution of impacts. We can however identify robust findings that prevail across different protection scenarios and socioeconomic conditions.

Our results suggest that conserving annual volumes of water for EFP can be achieved without major losses of forests and other unmanaged land at the global level. Socioeconomic changes have been shown to put considerably higher pressure on land resources than EFP does. This indicates that EFP is not fundamentally in opposition to sustainable land management at the global scale. Limiting the negative feedback of EFP on land ecosystems will likely require agricultural intensification on existing cropland. Such intensification should target productivity of all production factors including water and nutrients in order to avoid negative environmental impacts. In this context, it is positive that agricultural research and development is increasingly focusing on reducing the environmental impacts of intensive agriculture (Alston et al., 2009).

From a local perspective, changes in comparative advantages, associated production reallocation and local hotspots of land-use change may have a strong influence on livelihoods and environmental sustainability. We estimate that securing annual volumes of water for EFP mainly leads to cropland expansion into natural land ecosystems in locations where agricultural water-use is not directly affected by EFP. This indicates that a river basin perspective on water management as advocated by Lawford et al. (2013) may miss land-use feedbacks that can put the sustainability of local water management strategies into question. Furthermore, recent distortions of the global food market have resulted in food self-sufficiency programs in several countries including India, Japan and Qatar (Fader et al., 2013). In this context, our result that EFP may lead to production reallocation away from water scarce regions gives rise to the concern that regional and local food self-sufficiency ambitions may hamper the implementation of EFP policies.

In summary, our results indicate that global reservation of annual volumes of water for EFP can be achieved at moderate consequences for land resources. In reality, water is however managed by local or national authorities. Concerns about production reallocation and local land-use implications may therefore prevent EFP implementation.

Acknowledgements

The authors would like to thank three anonymous reviewers for their valuable comments. The research leading to these results has received funding from European Community's Seventh Framework Program (FP7/2007-2013) under grant agreements n° 266992 (Global-IQ) and n° 308329 (ADVANCE). Additional funding was provided by the BMBF through the INNOVATE project (grant agreement 01LL0904D).

References

Alcamo, J., DÖLL, P., Henrichs, T., Kaspar, F., Lehner, B., RÖSCH, T., Siebert, S., 2003. Development and testing of the WaterGAP 2 global model of water use and availability. Hydrol. Sci. J. 48, 317–337.

Alcamo, J., Flörke, M., Märker, M., 2007. Future long-term changes in global water resources driven by socio-economic and climatic changes. Hydrol. Sci. J. 52, 247–275. doi:10.1623/hysj.52.2.247

Alston, J.M., Beddow, J.M., Pardey, P.G., 2009. Agricultural research, productivity, and food prices in the long run. Science 325, 1209–1210.

Arthington, A.H., Bunn, S.E., Poff, N.L., Naiman, R.J., 2006. THE CHALLENGE OF PROVIDING ENVIRONMENTAL FLOW RULES TO SUSTAIN RIVER ECOSYSTEMS. Ecol. Appl. 16, 1311–1318. doi:10.1890/1051-0761(2006)016[1311:TCOPEF]2.0.CO;2

Arthington, A.H., Naiman, R.J., McCLAIN, M.E., Nilsson, C., 2010. Preserving the biodiversity and ecological services of rivers: new challenges and research opportunities: Preserving the biodiversity and ecological services of rivers. Freshw. Biol. 55, 1–16. doi:10.1111/j.1365-2427.2009.02340.x

Barlow, J., Gardner, T.A., Araujo, I.S., Ávila-Pires, T.C., Bonaldo, A.B., Costa, J.E., Esposito, M.C., Ferreira, L.V., Hawes, J., Hernandez, M.I., 2007. Quantifying the biodiversity value of tropical primary, secondary, and plantation forests. Proc. Natl. Acad. Sci. 104, 18555–18560.

Bennett, E.M., Peterson, G.D., Gordon, L.J., 2009. Understanding relationships among multiple ecosystem services: Relationships among multiple ecosystem services. Ecol. Lett. 12, 1394–1404. doi:10.1111/j.1461-0248.2009.01387.x

Biemans, H., Haddeland, I., Kabat, P., Ludwig, F., Hutjes, R.W.A., Heinke, J., von Bloh, W., Gerten, D., 2011. Impact of reservoirs on river discharge and irrigation water supply during the 20th century. Water Resour. Res. 47, n/a–n/a. doi:10.1029/2009WR008929

Bodirsky, B., Rolinski, S., Biewald, A., Weindl, I., Popp, A., Lotze-Campen, H., under review. Food Demand Projections for the 21st Century. Rev. Food Secur.

Bodirsky, B.L., Popp, A., Weindl, I., Dietrich, J.P., Rolinski, S., Scheiffele, L., Schmitz, C., Lotze-Campen, H., 2012. N2O emissions from the global agricultural nitrogen cycle – current state and future scenarios. Biogeosciences 9, 4169–4197. doi:10.5194/bg-9-4169-2012

Bondeau, A., Smith, P.C., Zaehle, S., Schaphoff, S., Lucht, W., Cramer, W., Gerten, D., Lotze-Campen, H., Mueller, C., Reichstein, M., Smith, B., 2007. Modelling the role of agriculture for the 20th century global terrestrial carbon balance. Glob. Change Biol. 13, 679–706. doi:10.1111/j.1365-2486.2006.01305.x

Calzadilla, A., Rehdanz, K., Tol, R.S.J., 2011. The GTAP-W model: Accounting for water use in agriculture (Kiel Working Papers No. 1745). Kiel Institute for the World Economy (IfW), Kiel.

Chaturvedi, V., Hejazi, M., Edmonds, J., Clarke, L., Kyle, P., Davies, E., Wise, M., 2013. Climate mitigation policy implications for global irrigation water demand. Mitig. Adapt. Strateg. Glob. Change. doi:10.1007/s11027-013-9497-4

De Fraiture, C., Wichelns, D., 2010. Satisfying future water demands for agriculture. Agric. Water Manag. 97, 502–511. doi:10.1016/j.agwat.2009.08.008

Dietrich, J.P., Popp, A., Lotze-Campen, H., 2013a. Reducing the loss of information and gaining accuracy with clustering methods in a global land-use model. Ecol. Model. 263, 233–243. doi:10.1016/j.ecolmodel.2013.05.009

Dietrich, J.P., Schmitz, C., Lotze-Campen, H., Popp, A., Mueller, C., 2013b. Forecasting technological change in agriculture - An endogenous implementation in a global land use model. Technol. Forecast. Soc. Change.

Dietrich, J.P., Schmitz, C., Müller, C., Fader, M., Lotze-Campen, H., Popp, A., 2012. Measuring agricultural land-use intensity – A global analysis using a model-assisted approach. Ecol. Model. 232, 109–118. doi:10.1016/j.ecolmodel.2012.03.002

Döll, P., Lehner, B., 2002. Validation of a new global 30-min drainage direction map. J. Hydrol. 258, 214–231.

Dudgeon, D., Arthington, A.H., Gessner, M.O., Kawabata, Z.-I., Knowler, D.J., Lévêque, C., Naiman, R.J., Prieur-Richard, A.-H., Soto, D., Stiassny, M.L.J., Sullivan, C.A., 2006.

Freshwater biodiversity: importance, threats, status and conservation challenges. Biol. Rev. 81, 163. doi:10.1017/S1464793105006950

Elliott, J., Deryng, D., Muller, C., Frieler, K., Konzmann, M., Gerten, D., Glotter, M., Florke, M., Wada, Y., Best, N., Eisner, S., Fekete, B.M., Folberth, C., Foster, I., Gosling, S.N., Haddeland, I., Khabarov, N., Ludwig, F., Masaki, Y., Olin, S., Rosenzweig, C., Ruane, A.C., Satoh, Y., Schmid, E., Stacke, T., Tang, Q., Wisser, D., 2013. Constraints and potentials of future irrigation water availability on agricultural production under climate change. Proc. Natl. Acad. Sci. doi:10.1073/pnas.1222474110

Erb, K.H., Gaube, V., Krausmann, F., Plutzar, C., Bondeau, A., Haberl, H., 2007. A comprehensive global 5 min resolution land-use data set for the year 2000 consistent with national census data. J. Land Use Sci. 2, 191–224+.

Fader, M., Gerten, D., Krause, M., Lucht, W., Cramer, W., 2013. Spatial decoupling of agricultural production and consumption: quantifying dependences of countries on food imports due to domestic land and water constraints. Environ. Res. Lett. 8, 014046. doi:10.1088/1748-9326/8/1/014046

Falkenmark, M., Molden, D., 2008. Wake Up to Realities of River Basin Closure. Int. J. Water Resour. Dev. 24, 201–215. doi:10.1080/07900620701723570

Falkenmark, M., Rockström, J., Karlberg, L., 2009. Present and future water requirements for feeding humanity. Food Secur. 1, 59–69. doi:10.1007/s12571-008-0003-x

FAO, 2010. Global forest resources assessment 2010: Main report. Food and Agriculture Organization of the United Nations.

FAOSTAT, 2005. Database Collection of the Food and Agriculture Organization of the United Nations.

FAOSTAT, 2013. Database Collection of the Food and Agriculture Organization of the United Nations.

Fischer, R.A., Edmeades, G.O., 2010. Breeding and Cereal Yield Progress. Crop Sci. 50, S–85–S–98. doi:10.2135/cropsci2009.10.0564

Flörke, M., Kynast, E., Bärlund, I., Eisner, S., Wimmer, F., Alcamo, J., 2013. Domestic and industrial water uses of the past 60 years as a mirror of socio-economic development: A global simulation study. Glob. Environ. Change 23, 144–156. doi:10.1016/j.gloenvcha.2012.10.018

Foley, J.A., Ramankutty, N., Brauman, K.A., Cassidy, E.S., Gerber, J.S., Johnston, M., Mueller, N.D., O'Connell, C., Ray, D.K., West, P.C., Balzer, C., Bennett, E.M., Carpenter, S.R., Hill, J., Monfreda, C., Polasky, S., Rockström, J., Sheehan, J., Siebert, S., Tilman, D., Zaks, D.P.M., 2011. Solutions for a cultivated planet. Nature 478, 337–342. doi:10.1038/nature10452

Ford, R.M., Williams, K.J.H., Bishop, I.D., Webb, T., 2009. A value basis for the social acceptability of clearfelling in Tasmania, Australia. Landsc. Urban Plan. 90, 196–206. doi:10.1016/j.landurbplan.2008.11.006

Gerten, D., Hoff, H., Rockström, J., Jägermeyr, J., Kummu, M., Pastor, A.V., 2013. Towards a revised planetary boundary for consumptive freshwater use: role of environmental flow requirements. Curr. Opin. Environ. Sustain. 5, 551 – 558. doi:http://dx.doi.org/10.1016/j.cosust.2013.11.001

Godfray, H.C.J., Beddington, J.R., Crute, I.R., Haddad, L., Lawrence, D., Muir, J.F., Pretty, J., Robinson, S., Thomas, S.M., Toulmin, C., 2010. Food Security: The Challenge of Feeding 9 Billion People. Science 327, 812–818. doi:10.1126/science.1185383

Grafton, R.Q., Pittock, J., Davis, R., Williams, J., Fu, G., Warburton, M., Udall, B., McKenzie, R., Yu, X., Che, N., Connell, D., Jiang, Q., Kompas, T., Lynch, A., Norris, R., Possingham, H., Quiggin, J., 2012. Global insights into water resources, climate change and governance. Nat. Clim. Change 3, 315–321. doi:10.1038/nclimate1746

Gupta, J., Pahl-Wostl, C., Zondervan, R., 2013. "Glocal" water governance: a multi-level challenge in the anthropocene. Curr. Opin. Environ. Sustain. 5, 573–580. doi:10.1016/j.cosust.2013.09.003

Hanasaki, N., Kanae, S., Oki, T., Masuda, K., Motoya, K., Shirakawa, N., Shen, Y., Tanaka, K., 2008. An integrated model for the assessment of global water resources Part 1: Model description and input meteorological forcing. Hydrol. Earth Syst. Sci. 12, 1007–1025.

Hansen, M.C., Potapov, P.V., Moore, R., Hancher, M., Turubanova, S.A., Tyukavina, A., Thau, D., Stehman, S.V., Goetz, S.J., Loveland, T.R., Kommareddy, A., Egorov, A., Chini, L., Justice, C.O., Townshend, J.R.G., 2013. High-Resolution Global Maps of 21st-Century Forest Cover Change. Science 342, 850–853. doi:10.1126/science.1244693

Hoekstra, A.Y., 2010. The Global Dimension of Water Governance: Why the River Basin Approach Is No Longer Sufficient and Why Cooperative Action at Global Level Is Needed. Water 3, 21–46. doi:10.3390/w3010021

Hoekstra, A.Y., Mekonnen, M.M., Chapagain, A.K., Mathews, R.E., Richter, B.D., 2012. Global Monthly Water Scarcity: Blue Water Footprints versus Blue Water Availability. PLoS ONE 7, e32688. doi:10.1371/journal.pone.0032688

Hoff, H., 2009. Global water resources and their management. Curr. Opin. Environ. Sustain. 1, 141–147. doi:10.1016/j.cosust.2009.10.001

IIASA, 2013. SSP Database (version 0.93). International Institute for Applied Systems Analysis (IIASA).

Intergovernmental Panel on Climate Change, Working Group III, 2000. Emissions scenarios. a special report of IPCC Working Group III. Intergovernmental Panel on Climate Change, [Geneva].

Jones, W.I., 1995. The World Bank and Irrigation.

Kijne, J.W., Barker, R., Molden, D., 2004. Water Productivity in Agriculture: Limits and Opportunities for Improvement. Cab Intl.

Klein Goldewijk, K., Beusen, A., Van Drecht, G., De Vos, M., 2011. The HYDE 3.1 spatially explicit database of human-induced global land-use change over the past 12,000 years: HYDE 3.1 Holocene land use. Glob. Ecol. Biogeogr. 20, 73–86. doi:10.1111/j.1466-8238.2010.00587.x

Klink, C.A., Machado, R.B., 2005. Conservation of the Brazilian cerrado. Conserv. Biol. 19, 707–713.

Krause, M., Lotze-Campen, H., Popp, A., Dietrich, J.P., Bonsch, M., 2013. Conservation of undisturbed natural forests and economic impacts on agriculture. Land Use Policy 30, 344–354. doi:10.1016/j.landusepol.2012.03.020

Lambin, E.F., Meyfroidt, P., 2011. Inaugural Article: Global land use change, economic globalization, and the looming land scarcity. Proc. Natl. Acad. Sci. 108, 3465–3472. doi:10.1073/pnas.1100480108

Lawford, R., Bogardi, J., Marx, S., Jain, S., Wostl, C.P., Knüppe, K., Ringler, C., Lansigan, F., Meza, F., 2013. Basin perspectives on the Water–Energy–Food Security Nexus. Curr. Opin. Environ. Sustain. 5, 607–616. doi:10.1016/j.cosust.2013.11.005

Lotze-Campen, H., Müller, C., Bondeau, A., Rost, S., Popp, A., Lucht, W., 2008. Global food demand, productivity growth, and the scarcity of land and water resources: a spatially explicit mathematical programming approach. Agric. Econ. 39, 325–338.

Lotze-Campen, H., Popp, A., Beringer, T., Müller, C., Bondeau, A., Rost, S., Lucht, W., 2010. Scenarios of global bioenergy production: The trade-offs between agricultural expansion, intensification and trade. Ecol. Model. 221, 2188–2196. doi:10.1016/j.ecolmodel.2009.10.002

Mitchell, T.D., Jones, P.D., 2005. An improved method of constructing a database of monthly climate observations and associated high-resolution grids. Int. J. Climatol. 25, 693–712. doi:10.1002/joc.1181

Molden, D., Oweis, T., Steduto, P., Bindraban, P., Hanjra, M.A., Kijne, J., 2010. Improving agricultural water productivity: Between optimism and caution. Agric. Water Manag. 97, 528–535. doi:10.1016/j.agwat.2009.03.023

Müller, C., Robertson, R.D., 2013. Projecting future crop productivity for global economic modeling. Agric. Econ. in press.

Narayanan, G. Badri, Terry L. Walmsley, 2008. Global Trade, Assistance, and Production: The GTAP 7 Data Base.

Naughton-Treves, L., Holland, M.B., Brandon, K., 2005. THE ROLE OF PROTECTED AREAS IN CONSERVING BIODIVERSITY AND SUSTAINING LOCAL LIVELIHOODS. Annu. Rev. Environ. Resour. 30, 219–252. doi:10.1146/annurev.energy.30.050504.164507

Naylor, 1996. ENERGY AND RESOURCE CONSTRAINTS ON INTENSIVE AGRICULTURAL PRODUCTION. Annu Rev Energy Env.

Oki, T., 2006. Global Hydrological Cycles and World Water Resources. Science 313, 1068–1072. doi:10.1126/science.1128845

Onaindia, M., Fernández de Manuel, B., Madariaga, I., Rodríguez-Loinaz, G., 2013. Co-benefits and trade-offs between biodiversity, carbon storage and water flow regulation. For. Ecol. Manag. 289, 1–9. doi:10.1016/j.foreco.2012.10.010

Pahl-Wostl, C., Arthington, A., Bogardi, J., Bunn, S.E., Hoff, H., Lebel, L., Nikitina, E., Palmer, M., Poff, L.N., Richards, K., Schlüter, M., Schulze, R., St-Hilaire, A., Tharme, R., Tockner, K., Tsegai, D., 2013a. Environmental flows and water governance: managing sustainable water uses. Curr. Opin. Environ. Sustain. 5, 341–351. doi:10.1016/j.cosust.2013.06.009

Pahl-Wostl, C., Palmer, M., Richards, K., 2013b. Enhancing water security for the benefits of humans and nature—the role of governance. Curr. Opin. Environ. Sustain. 5, 676–684. doi:10.1016/j.cosust.2013.10.018

Pahl-Wostl, C., Vörösmarty, C., Bhaduri, A., Bogardi, J., Rockström, J., Alcamo, J., 2013c. Towards a sustainable water future: shaping the next decade of global water research. Curr. Opin. Environ. Sustain. 5, 708–714. doi:10.1016/j.cosust.2013.10.012

Palanisami, K., 1997. Irrigation Technology Transfer in Support of Food Security.

Pardey, P.G., Alston, J.M., Piggott, R., 2006. Agricultural R & D in the developing world: too little, too late? International Food Policy Research Institute (IFPRI), Washington, D.C.

Pastor, A.V., Ludwig, F., Biemans, H., Hoff, H., Kabat, P., 2013. Accounting for environmental flow requirements in global water assessments. Hydrol. Earth Syst. Sci. Discuss. 10, 14987–15032. doi:10.5194/hessd-10-14987-2013

Poff, N.L., Richter, B.D., Arthington, A.H., Bunn, S.E., Naiman, R.J., Kendy, E., Acreman, M., Apse, C., Bledsoe, B.P., Freeman, M.C., Henriksen, J., Jacobson, R.B., Kennen, J.G., Merritt, D.M., Oâ€ ™KEEFFE, J.H., Olden, J.D., Rogers, K., Tharme, R.E., Warner, A., 2010. The ecological limits of hydrologic alteration (ELOHA): a new framework for developing regional environmental flow standards: Ecological limits of hydrologic alteration. Freshw. Biol. 55, 147–170. doi:10.1111/j.1365-2427.2009.02204.x

Popp, A., Lotze-Campen, H., Bodirsky, B., 2010. Food consumption, diet shifts and associated non-CO2 greenhouse gases from agricultural production. Glob. Environ. Change 20, 451 – 462. doi:10.1016/j.gloenvcha.2010.02.001

Portmann, F.T., Siebert, S., Döll, P., 2010. MIRCA2000-Global monthly irrigated and rainfed crop areas around the year 2000: A new high-resolution data set for agricultural and hydrological modeling. Glob. Biogeochem. Cycles 24, GB1011.

Postel, S.L., Daily, G.C., Ehrlich, P.R., 1996. Human Appropriation of Renewable Fresh Water. Science 271, 785–788. doi:10.1126/science.271.5250.785

Revenga, C., Smakhtin, V., Doll, P., Comprehensive Assessment Secretariat -Colombo, L.K., 2004. Taking into account environmental water requirements in global-scale water resources assessments, Research report / IWMI. Comprehensive Assessment Secretariat, Colombo, Sri Lanka.

Ringler, C., Bhaduri, A., Lawford, R., 2013. The nexus across water, energy, land and food (WELF): potential for improved resource use efficiency? Curr. Opin. Environ. Sustain. 5, 617–624. doi:10.1016/j.cosust.2013.11.002

Rohwer, J., Gerten, D., Lucht, W., 2007. DEVELOPMENT OF FUNCTIONAL IRRIGATION TYPES FOR IMPROVED GLOBAL CROP MODELLING.

Rosegrant, M.W., Ringler, C., Zhu, T., 2009. Water for agriculture: maintaining food security under growing scarcity. Annu. Rev. Environ. Resour. 34, 205–222.

Rost, S., Gerten, D., Bondeau, A., Lucht, W., Rohwer, J., Schaphoff, S., 2008. Agricultural green and blue water consumption and its influence on the global water system. Water Resour Res 44.

Sauer, T., Havlík, P., Schneider, U.A., Schmid, E., Kindermann, G., Obersteiner, M., 2010. Agriculture and resource availability in a changing world: The role of irrigation. Water Resour. Res. 46, W06503.

Schaible, G., Aillery, M., 2013. Western Irrigated Agriculture: Production Value, Water Use, Costs, and Technology Vary by Farm Size.

Schewe, J., Heinke, J., Gerten, D., Haddeland, I., Arnell, N.W., Clark, D.B., Dankers, R., Eisner, S., Fekete, B.M., Colon-Gonzalez, F.J., Gosling, S.N., Kim, H., Liu, X., Masaki, Y., Portmann, F.T., Satoh, Y., Stacke, T., Tang, Q., Wada, Y., Wisser, D., Albrecht, T., Frieler, K., Piontek, F., Warszawski, L., Kabat, P., 2013. Multimodel assessment of water scarcity under climate change. Proc. Natl. Acad. Sci. doi:10.1073/pnas.1222460110

Schmitz, C., Biewald, A., Lotze-Campen, H., Popp, A., Dietrich, J.P., Bodirsky, B., Krause, M., Weindl, I., 2012. Trading more food: Implications for land use, greenhouse gas emissions, and the food system. Glob. Environ. CHANGE-Hum. POLICY Dimens. 22, 189–209. doi:10.1016/j.gloenvcha.2011.09.013

Schmitz, C., van Meijl, H., Kyle, P., Nelson, G.C., Fujimori, S., Gurgel, A., Havlik, P., Heyhoe, E., d’ Croz, D.M., Popp, A., Sands, R., Tabeau, A., van der Mensbrugghe, D., von Lampe, M., Wise, M., Blanc, E., Hasegawa, T., Kavallari, A., Valin, H., 2014. Land-use change trajectories up to 2050: insights from a global agro-economic model comparison. Agric. Econ. 45, 69–84. doi:10.1111/agec.12090

Seppelt, R., Lautenbach, S., Volk, M., 2013. Identifying trade-offs between ecosystem services, land use, and biodiversity: a plea for combining scenario analysis and optimization on different spatial scales. Curr. Opin. Environ. Sustain. 5, 458–463. doi:10.1016/j.cosust.2013.05.002

Shen, Y., Oki, T., Utsumi, N., KANAE, S., HANASAKI, N., 2008. Projection of future world water resources under SRES scenarios: water withdrawal / Projection des ressources en eau mondiales futures selon les scénarios du RSSE: prélèvement d'eau. Hydrol. Sci. J. 53, 11–33. doi:10.1623/hysj.53.1.11

Shiklomanov, I.A., 2000. Appraisal and Assessment of World Water Resources. Water Int. 25, 11–32. doi:10.1080/02508060008686794

Siebert, S., Doell, P., Feick, S., Hoogeveen, J., Frenken, K., 2007. Global Map of Irrigation Areas version 4.0.1.

Siebert, S., Döll, P., 2007. Irrigation water use – A global perspective. Water Resour. Res. 38. doi:10.1029/2001WR000355

Smakhtin, V., Revenga, C., Döll, P., 2004. A pilot global assessment of environmental water requirements and scarcity. Water Int. 29, 307–317.

Smakhtin, V.U., Eriyagama, N., 2008. Developing a software package for global desktop assessment of environmental flows. Environ. Model. Softw. 23, 1396–1406. doi:10.1016/j.envsoft.2008.04.002

Smeets, E.M.W., Faaij, A.P.C., 2007. Bioenergy potentials from forestry in 2050: An assessment of the drivers that determine the potentials. Clim. Change 81, 353–390. doi:10.1007/s10584-006-9163-x

Smith, P., Gregory, P.J., van Vuuren, D., Obersteiner, M., Havlik, P., Rounsevell, M., Woods, J., Stehfest, E., Bellarby, J., 2010. Competition for land. Philos. Trans. R. Soc. B Biol. Sci. 365, 2941–2957. doi:10.1098/rstb.2010.0127

Smith, P., Haberl, H., Popp, A., Erb, K., Lauk, C., Harper, R., Tubiello, F., de Siqueira Pinto, A., Jafari, M., Sohi, S., Masera, O., Böttcher, H., Berndes, G., Bustamante, M., Ahammad, H., Clark, H., Dong, H., Elsiddig, E.A., Mbow, C., Ravindranath, N.H., Rice, C.W., Robledo-Abad, C., Romanovskaya, A., Sperling, F., Herrero, M., House, J.I., Rose, S., 2013. How much land based greenhouse gas mitigation can be achieved without compromising food security and environmental goals? Glob. Change Biol. n/a–n/a. doi:10.1111/gcb.12160

Strzepek, K., Boehlert, B., 2010. Competition for water for the food system. Philos Trans R Soc Lond B Biol Sci 365, 2927–40. doi:Review

Tennant, D.L., 1976. Instream Flow Regimens for Fish, Wildlife, Recreation and Related Environmental Resources. Fisheries 1, 6–10. doi:10.1577/1548-8446(1976)001<0006:IFRFFW>2.0.CO;2

UNESCO, 2009. The United Nations world water development report 3.

Vorosmarty, C.J., McIntyre, P.B., Gessner, M.O., Dudgeon, D., Prusevich, A., Green, P., Glidden, S., Bunn, S.E., Sullivan, C.A., Liermann, C.R., Davies, P.M., 2010. Global threats to human water security and river biodiversity. Nature 467, 555–561. doi:10.1038/nature09440

Wada, Y., van Beek, L.P.H., Viviroli, D., Dürr, H.H., Weingartner, R., Bierkens, M.F.P., 2011. Global monthly water stress: 2. Water demand and severity of water stress. Water Resour. Res. 47, n/a–n/a. doi:10.1029/2010WR009792

Wisser, D., Frolking, S., Douglas, E.M., Fekete, B.M., Vörösmarty, C.J., Schumann, A.H., 2008. Global irrigation water demand: Variability and uncertainties arising from agricultural and climate data sets. Geophys. Res. Lett. 35. doi:10.1029/2008GL035296

Appendix

Appendix A: Additional methods and scenario descriptions

A.1 MAgPIE regions and simulation units

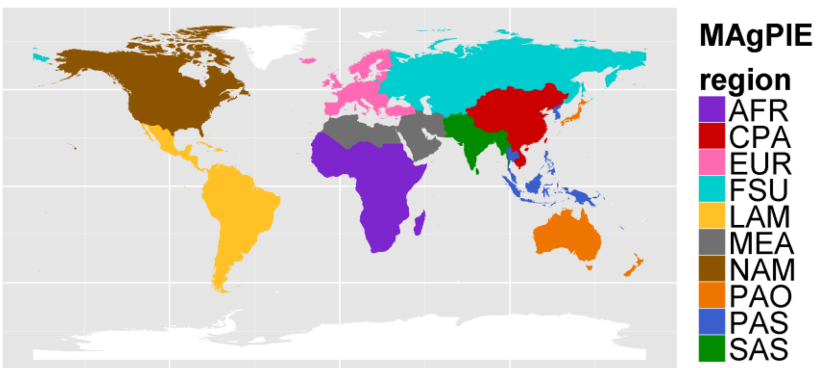

Figure A1 MAgPIE world regions. AFR=Sub Saharan Africa, CPA= centrally planned Asia, EUR=Europe, FSU=former Soviet Union, LAM=Latin America, MEA=Middle East and North Africa, NAM=North America, PAO=Pacific OECD, PAS=Pacific Asia, SAS=South Asia. Greenland and Antarctica are not covered by MAgPIE.

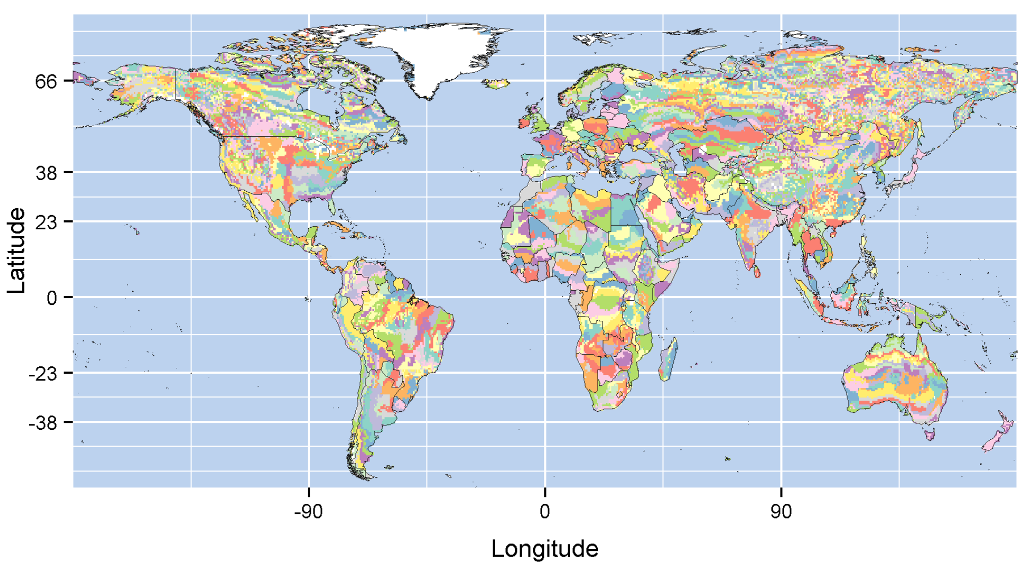

Figure A2 MAgPIE simulation units. The 1000 simulation units are aggregates of 0.5 x 0.5 latitude/longitude grid cells based on similarity of biophysical conditions (Dietrich et al., 2013a) and differ in size.

A.2 Irrigation costs

We use the rent associated with irrigation water application (i.e. factor payments for irrigation water) as a proxy for the annual factor requirement costs of irrigation. In order to derive the rent of irrigation water application from the GTAP land rent (Narayanan et al., 2008), we largely follow an approach by (Calzadilla et al., 2011).

In a first step, the ratio of irrigated production (prod_ir) to total production (prod_tot) based on LPJmL yields and the crop pattern from the MIRCA dataset (Portmann et al., 2010) is calculated. This share is multiplied by the total land rent from GTAP (R_tot) to obtain the land rent of irrigated production (R_ir) (equation A1). The calculation is done for all GTAP crop categories (crop) and countries (cntr) separately.

$$R_{ir(cntr,crop)} = \frac{prod_{ir}(cntr,crop)}{prod_{tot}(cntr,crop)} * R_{tot}(cntr,crop) \qquad (A1)$$

Using physical production as a weight for splitting the land rent assumes that the economic value is equal for all units produced.

This is usually not the case as prices for agricultural products vary strongly over the season. For instance, irrigation is often used to increase production of a commodity at a time when it is scarce and the price is high. This leads to a higher economic value of irrigation than physical production numbers would suggest. As a result, our approach may lead to a slight underestimation of the land rent associated with irrigated production.

In a second step, the land rent of irrigated production is further split into the value share of irrigable land (R_{ir}^{land}) and the value share of irrigation water (R_{ir}^{wat}). To calculate R_{ir}^{land}, we use the ratio of rainfed and irrigated yields Y_{rf} and Y_{ir} and multiply it with the total rent of irrigated production (equation A2).

$$R_{ir}^{land}(cntr,crop) = \frac{Y_{rf}(cntr,crop)}{Y_{ir}(cntr,crop)} R_{ir}(cntr,crop) \qquad (A2)$$

$$R_{ir}^{wat}(cntr,crop) = R_{ir}(cntr,crop) - R_{ir}^{land}(cntr,crop) \qquad (A3)$$

The rent associated with irrigable land (R_{ir}^{land}) can be interpreted as the rent that could have been obtained by doing rainfed production on the land actually used for irrigated production. The remainder (R_{ir}^{wat}) of the rent of irrigated production is consequently assigned to the actual application of irrigation water (equation A3). In reality, irrigation takes place in locations where the economic benefit is highest, i.e. where the ratio of rainfed to irrigated yields is low. Applying the mean country ratio of rainfed to irrigated yields therefore tends to overestimate the value of irrigable land R_{ir}^{land}. To avoid this bias, we refined the algorithm by using the yield ratio only on area equipped for irrigation (Siebert et al., 2007). Wherever there is no information available for a specific country - crop combination, the world average value of that crop is used for computation. Finally, the country values are aggregated to the MAgPIE regions using a production weighted mean and the GTAP crops are aggregated to the MAgPIE crop categories.

	1995	2005	2015	2025	2035	2045
AFR	37173	31444	25715	19986	14257	8528
CPA	8781	8214	7647	7080	6514	5947
EUR	5663	5663	5663	5663	5663	5663
FSU	5663	5663	5663	5663	5663	5663
LAM	12237	11042	9846	8651	7456	6261
MEA	5933	5884	5835	5786	5737	5688
NAM	5663	5663	5663	5663	5663	5663
PAO	5663	5663	5663	5663	5663	5663
PAS	2078	2730	3382	4033	4685	5337
SAS	1899	2584	3268	3952	4637	5321

Table A1: Investment costs for expanding irrigation infrastructure in US$ per hectare.

	AFR	CPA	EUR	FSU	LAM	MEA	NAM	PAO	PAS	SAS
temperate cereals	31	109	96	34	48	39	51	70	97	56
tropical cereals	10	71	67	11	30	22	52	52	30	15
maize	10	55	46	19	17	52	53	78	20	15
rice	26	118	117	43	48	123	88	195	57	57
others	83	441	295	187	178	273	482	965	138	203
potato	332	695	805	389	396	764	1098	2011	609	696
cassava	46	162	94	72	72	397	92	230	67	129
pulses	59	271	280	177	81	125	220	248	153	104
soybean	21	80	105	20	77	76	71	105	36	40
rapeseed	222	400	597	92	304	325	246	439	728	229
groundnut	36	188	119	87	70	193	120	175	66	66
sunflower	105	398	243	141	286	140	199	229	196	125
oil palm	75	381	193	193	266	193	193	193	278	193
sugar beet	77	65	111	37	117	80	84	212	77	56
sugar cane	218	401	321	319	287	883	301	765	318	361
cotton	60	280	256	145	111	284	127	423	200	103

Table A2: Annual factor requirement costs for irrigation for all regions and crops in US$ per hectare and year.

A.3 Environmental flow calculations

This is a detailed description of the calculations for available water and environmental water requirements. All hydrological data is obtained from LPJmL. The index j stands for the cell, b is for the river basin and m for the month. Hydrological data is provided by LPJmL.

The calculation of monthly available water, MAW(j,m), is done based on monthly discharge, Q(j,m), and monthly runoff, R(j,m), according to equation A4.

$$MAW(j,m) = \sum_{c\,\in b(j)} R(c,m) * \frac{Q(j,m)}{\sum_{c\in b(j)} Q(c,m)} \qquad (A4)$$

Monthly environmental flow requirements, EFR(j,m), for the Tennant method (Tennant, 1976) are calculated according to equation A5.

$$EFR(j,m) = \; MAW(j,m) * 0.3 \qquad (A5)$$

Monthly low-flow requirements for the Smakhtin (Smakhtin et al., 2004) method (LFR(j,m)) are calculated based on Q90(j), the 90 % quantile of monthly discharge over one year (equation A6).

$$LFR(j,m) = \; MAW(j,m) * \frac{\min\big(Q(j,m)\,,Q90(j,m)\big)}{Q(j,m)} \qquad (A6)$$

Associated high-flow requirements, HFR(j,m), are subsequently derived using equation A7.

$$HFR(j,m) = \begin{cases} 0{,}2 * MAW(j,m) & if \quad \frac{Q90(j,m)}{Q(j,m)} < 0.1 \\ 0{,}15 * MAW(j,m) & if \quad 0.1 \le \frac{Q90(j,m)}{Q(j,m)} < 0.2 \\ 0{,}07 * MAW(j,m) & if \quad 0.2 \le \frac{Q90(j,m)}{Q(j,m)} < 0.3 \end{cases} \qquad (A7)$$

Total monthly EFR are the sum of low and high flow components: EFR(j,m)= LFR(j,m) + HFR(j,m).

For the Hanasaki method (Hanasaki et al., 2008), calculations are based on QC(j,m) (in mm per month), the monthly discharge divided by the catchment area , i.e. the area of all upstream cells (according to personal communication with authors). As shown in Table 1, cells are classified into four categories according to minimum and maximum annual discharge. A category and cell specific fraction of available water F(j,m) is then used as the cellular environmental flow requirement (equation A8). The values for the protected fraction depend on monthly discharge and are shown in Table 1.

$$EFR(j,m) = MAW(j,m) * F(j,m) \qquad (A8)$$

Finally, annual environmental flow requirements AEFR(j) are obtained by summing the monthly values and truncating at 50% of annually available water based on (Revenga et al., 2004) (equation A9).

$$AEFR(j) = \min\left(0.5 * \sum_m MAW(j,m) \;, \sum_m EFR(j,m) \right) \qquad (A9)$$

A.4 Food, livestock and material demand

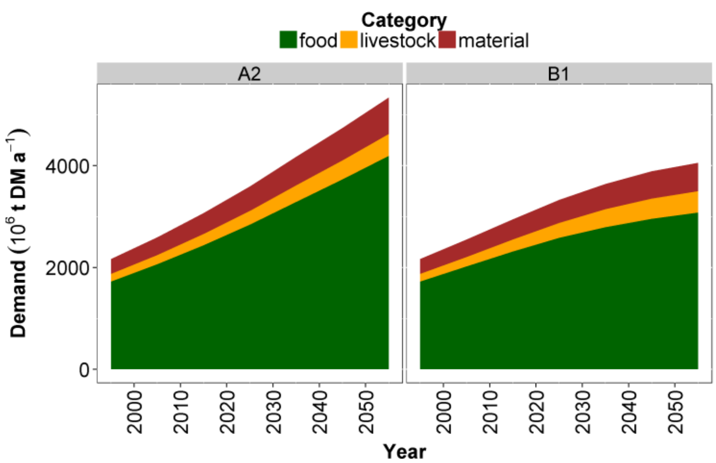

Figure A3 Global demand for vegetal food, livestock products and material for the two socioeconomic scenarios in million tons dry matter per year (Bodirsky et al., under review).

Appendix B: Additional model results for baseline runs

B.1 Agricultural water withdrawals

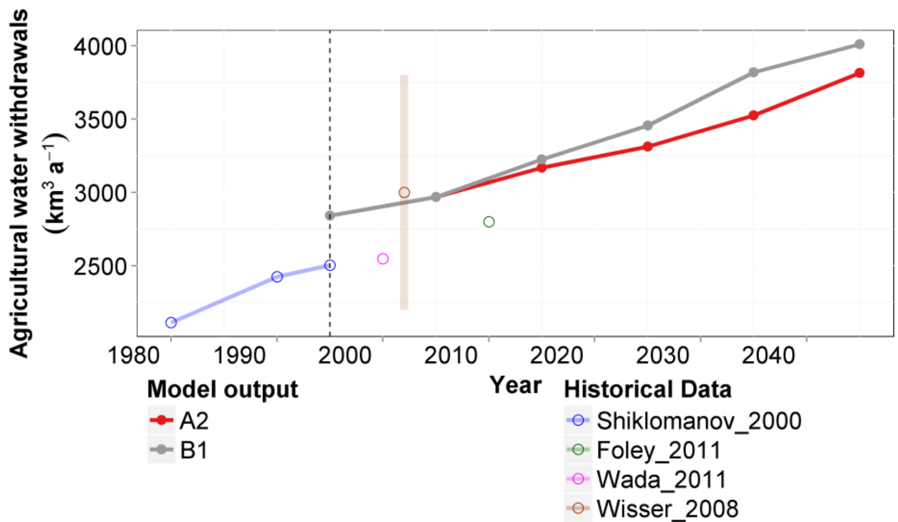

Figure B1 Global agricultural water withdrawals without EFP under the two socioeconomic scenarios. Estimates of historical and current agricultural water withdrawals by (Shiklomanov, 2000) (Shiklomanov_2000), (Foley et al., 2011) (Foley_2011), (Wada et al., 2011) (Wada_2011) and (Wisser et al., 2008) (Wisser_2008). The brown shaded bar corresponds to the uncertainty estimate provided by Wisser et al. A vertical dashed line marks the start of the simulation period.

Without environmental flow protection (EFP), increasing food demand leads to an increase of agricultural water withdrawals (AWW) from 2842 km^3 in 1995 to 3815 km^3 (A2) and 4010 km^3 (B1) in 2045 (Figure B1). Our base year estimate of agricultural water withdrawals is at the higher end of historical estimates. It is however well consistent with data provided by (Wisser et al., 2008) who used different irrigated area patterns and climate datasets to estimate AWW. The slope of our projection is similar to historical trends estimated by (Shiklomanov, 2000).

Even though food demand increases for the A2 scenario are stronger than for B1 (Figure B1), agricultural water withdrawals are higher in B1 by the mid of the century. The reason behind this behavior is the stronger increase in competing water uses under the A2 scenario (Figure 2) that limits the water available for agriculture. This is in contrast to results by (Shen et al., 2008), who project higher AWW in 2055 under the A2 scenario (4691 km^3) than under the B1 scenario (3683 km^3).Their analysis assumes constant irrigated area per capita and neglects water availability constraints and competing water demand from other sectors.

B.2 Irrigated area

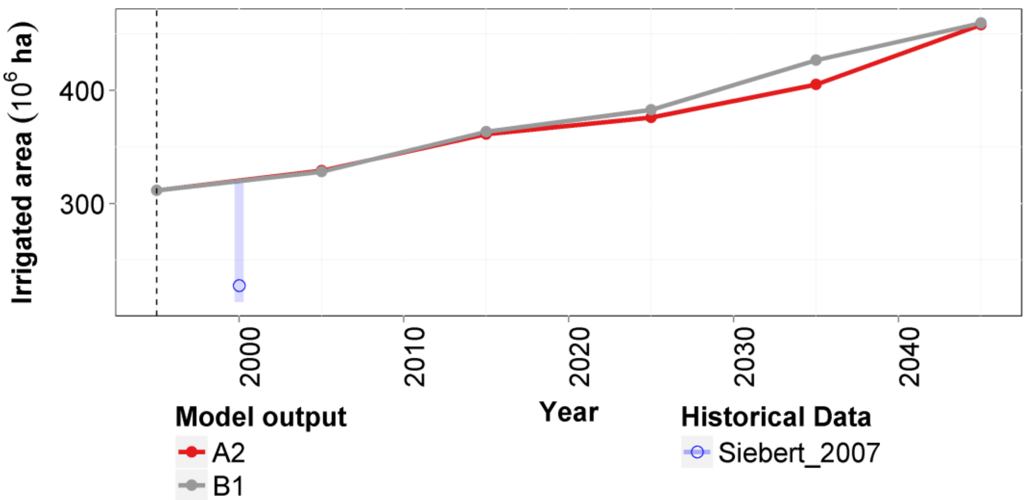

Figure B2 Global irrigated area development without EFP under the two socioeconomic scenarios. The blue shaded bar corresponds to the range of estimated historical irrigated area as reported by (Siebert and Döll, 2007) (Siebert_2007). A vertical dashed line marks the start of the simulation period.

Irrigated area develops similar to agricultural water withdrawals, increasing from 312 Mha in 1995 to 460 Mha in 2045 under both socioeconomic scenarios (Figure B2). Our initial irrigated area is at the higher end of the range of irrigated area estimates as reported by (Siebert and Döll, 2007). Irrigated area increases by ~ 20 % until 2025. This is slightly a stronger increase than found by (Sauer et al., 2010) who estimate irrigated area in 2030 to be 15% higher than in the year 2000. Even though agricultural water withdrawals differ between the two scenarios, crop- as well as location-specific irrigation water demand allows the model to optimize irrigation patterns so that total irrigated area is similar for both scenarios. Moreover, investments into technological change are higher in the A2 scenario (Figure B4) resulting in improved water use efficiency.

B.3 Cropland

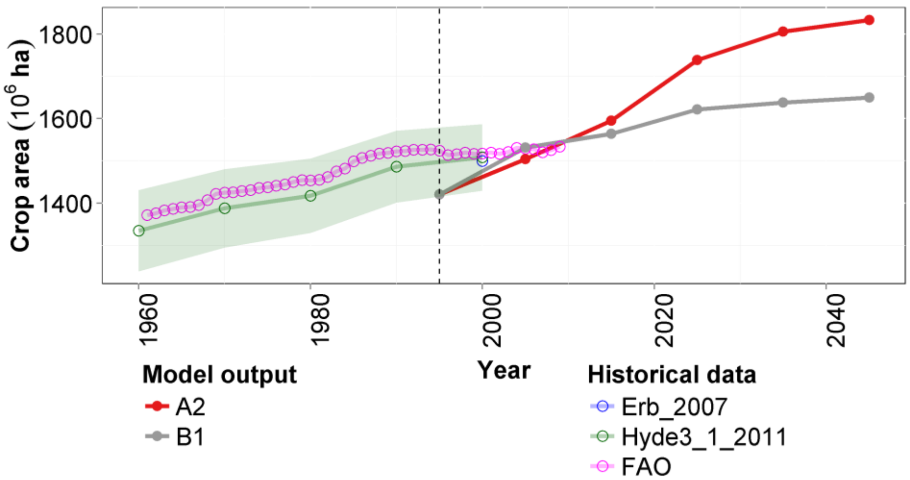

Figure B3 Global cropland development without EFP under the two socioeconomic scenarios. Estimates of historical cropland by (Erb et al., 2007) (Erb_2007, blue), (Klein Goldewijk et al., 2011) (Hyde3_1_2011, green with uncertainty range) and (FAOSTAT, 2013) (FAO, purple) for comparison. A vertical dashed line marks the start of the simulation period.

Global cropland projections for A2 are substantially higher than for B1 after 2015 (Figure B3) because of the stronger increase in food demand (Figure A2). Our base year cropland (1420 Mha) is calibrated to the average FAO cropland (category “Arable land and permanent crops”) for the period 1990 to 1999 (FAOSTAT, 2013) at regional level. Global cropland area reaches 1833 Mha in 2045 under the A2 scenario and 1650 Mha under B1.

B.4 Land-use intensity

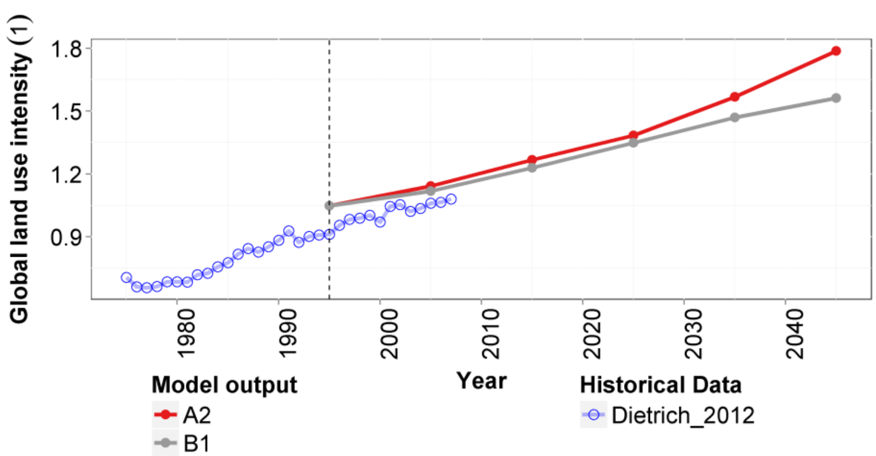

Figure B4 Global land-use intensity for the baseline scenarios without EFP. Increases over the simulation period reflect investments into yield increasing technological change (TC). Historical data from (Dietrich et al., 2013b). A vertical dashed line marks the start of the simulation period.

Global land-use intensity, i.e. global yield levels, increased by around 1.5 % per year between 1970 and 2007. In our projections, increases continue until the mid of the century at a rate of ~1% for A2 and 0.9 % for B1. This is lower than the increases we have seen in the past.

Appendix C: Additional model results on the effects of environmental flow protection

C.1 Regional changes in Agricultural water withdrawals due to environmental flow protection

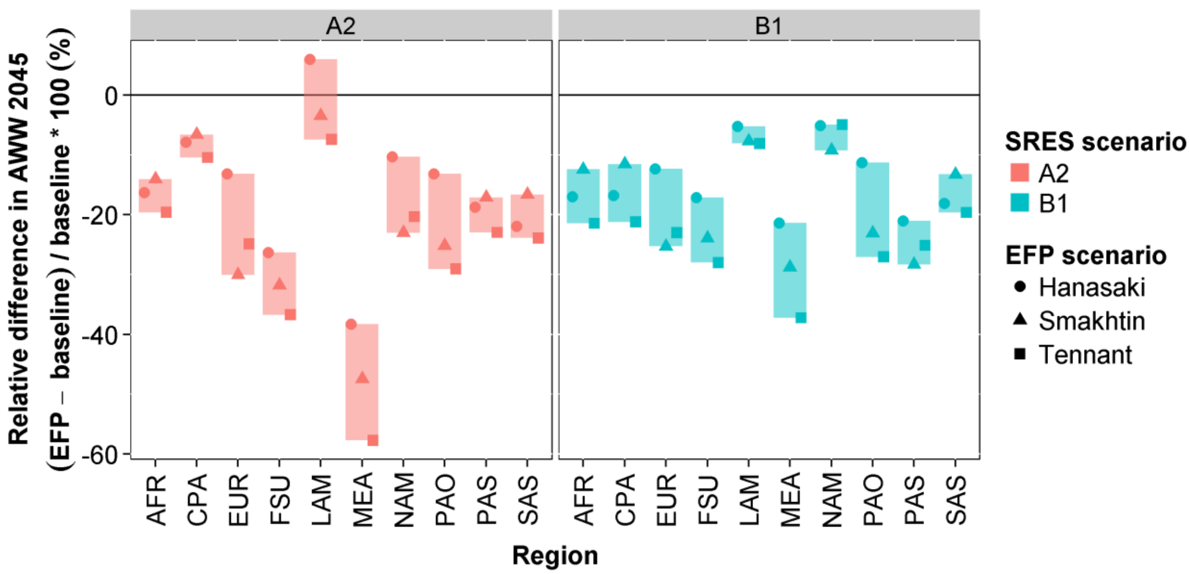

Figure C1 Regional changes in agricultural water withdrawals (AWW) due to EFP in 2045 relative to baseline agricultural water withdrawals for the two socioeconomic scenarios. Points indicate the value for the individual EFP scenarios. Shaded areas correspond to the whole range of changes due to EFP under each socioeconomic scenario.

C.2 Shadow prices for land

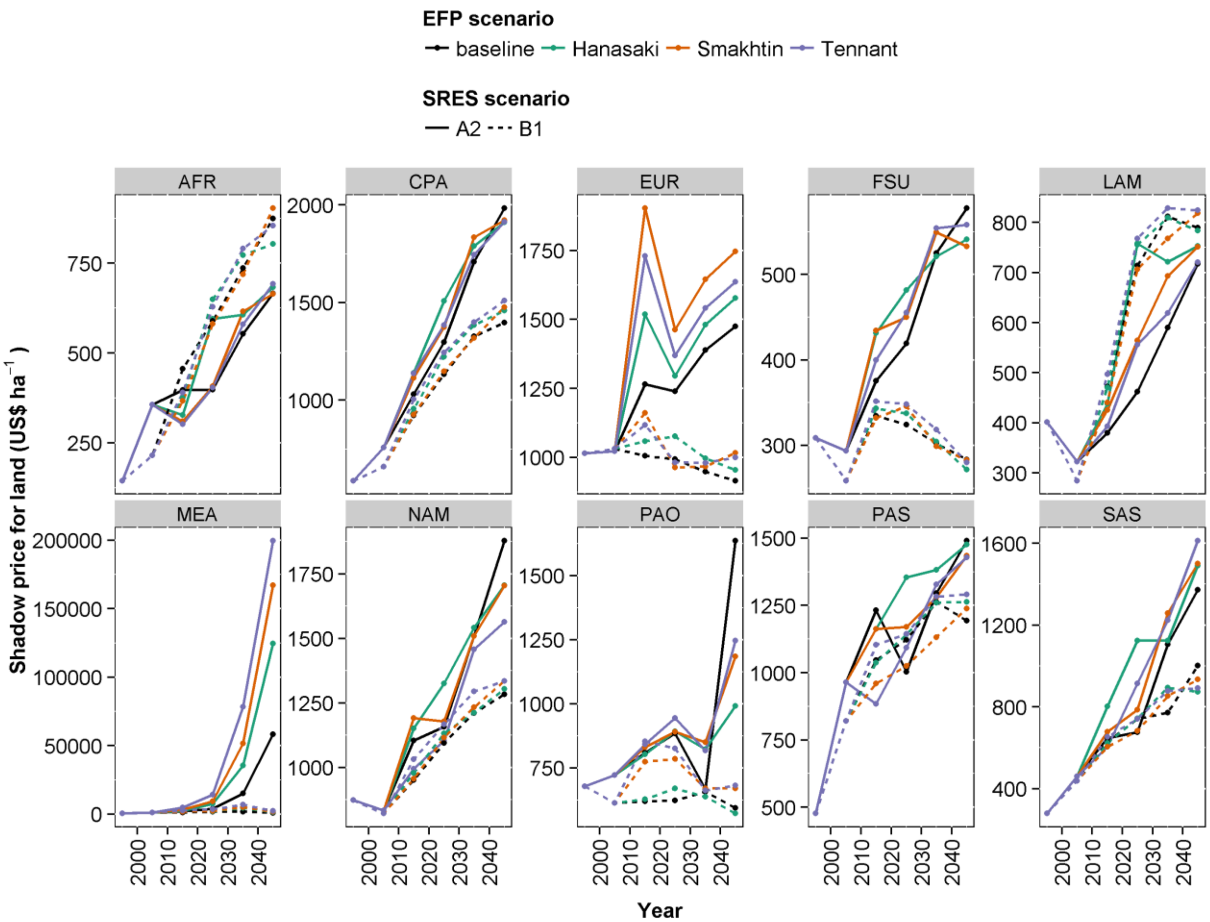

Figure C2 Average regional shadow prices for relaxing the land constraint by one unit. Shadow prices are aggregated to regional level using a cropland weighted mean.

C.3 Shadow prices for water

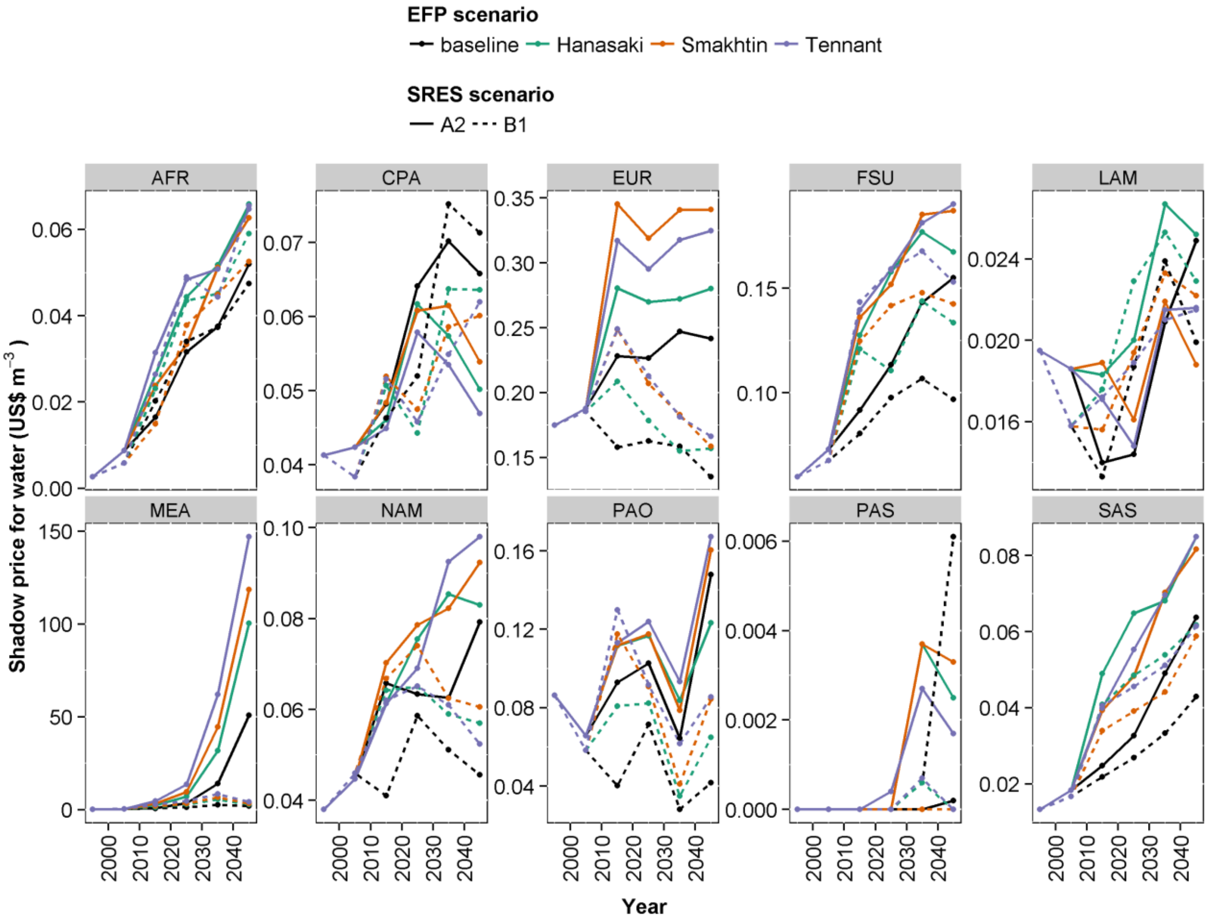

Figure C3 Average regional shadow prices for relaxing the water constraint by one unit. Aggregation to regional level using an agricultural water withdrawal weighted mean.

C.4 Regional land available for cropland expansion

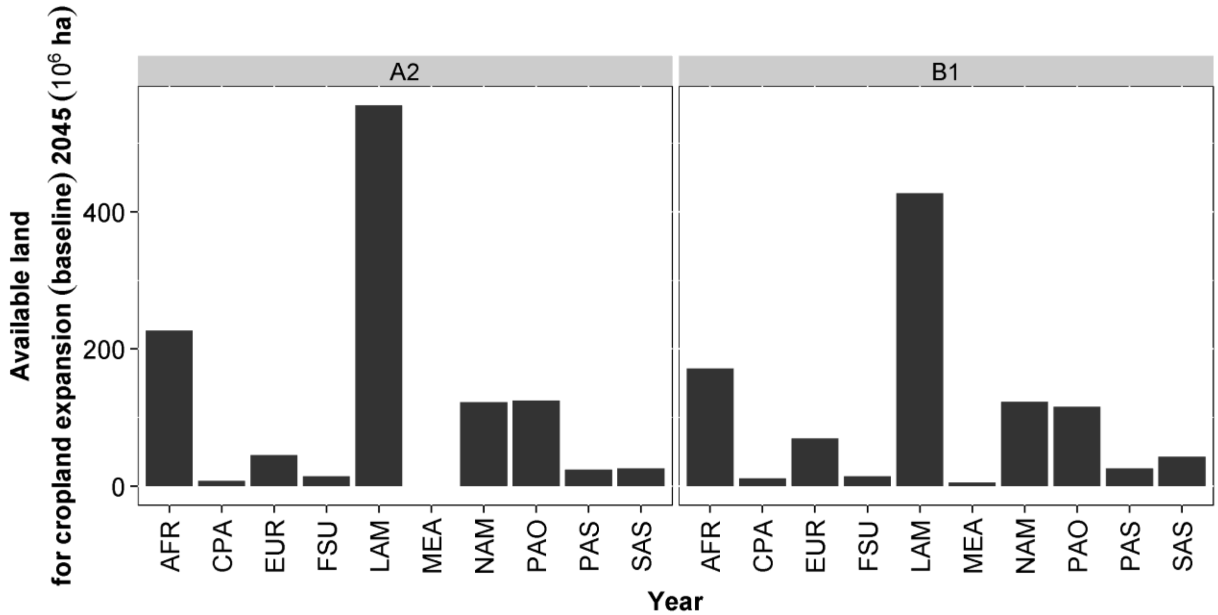

Figure C4 Regional land available for cropland expansion in 2045 in the baseline scenarios without EFP. Available land comprises unprotected natural forests (Section 2.2.2) and other unmanaged land.

C.5 Changes in regional production due to environmental flow protection

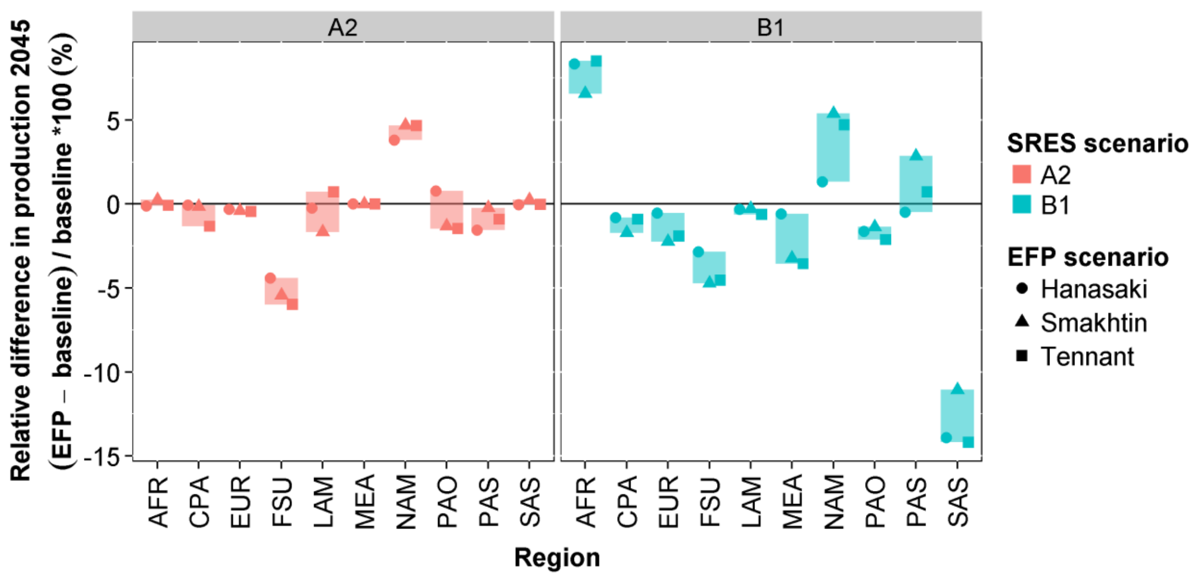

Figure C5 Regional changes in production due to EFP in 2045 relative to baseline production for the two socioeconomic scenarios. Points indicate the value for the individual EFP scenarios. Shaded areas correspond to the whole range of changes due to EFP under the respective socioeconomic scenario.

Appendix D: Sensitivity analysis

D.1 Technological change costs

Higher costs for yield increasing technological change (TC) amplify the effect of EFP on AWW (reductions due to EFP up to 1060 km^3; Figure D1, left) and cropland expansion (expansion due to EFP up to 80 Mha; Figure D1, right) under the A2 scenario. Cheaper TC leads to a reduction of EFP implications for AWW (reductions due to EFP up to 660 km^3) and cropland extent (expansion due to EFP up to 30 Mha). In B1, the difference between assumptions on TC costs is less pronounced.

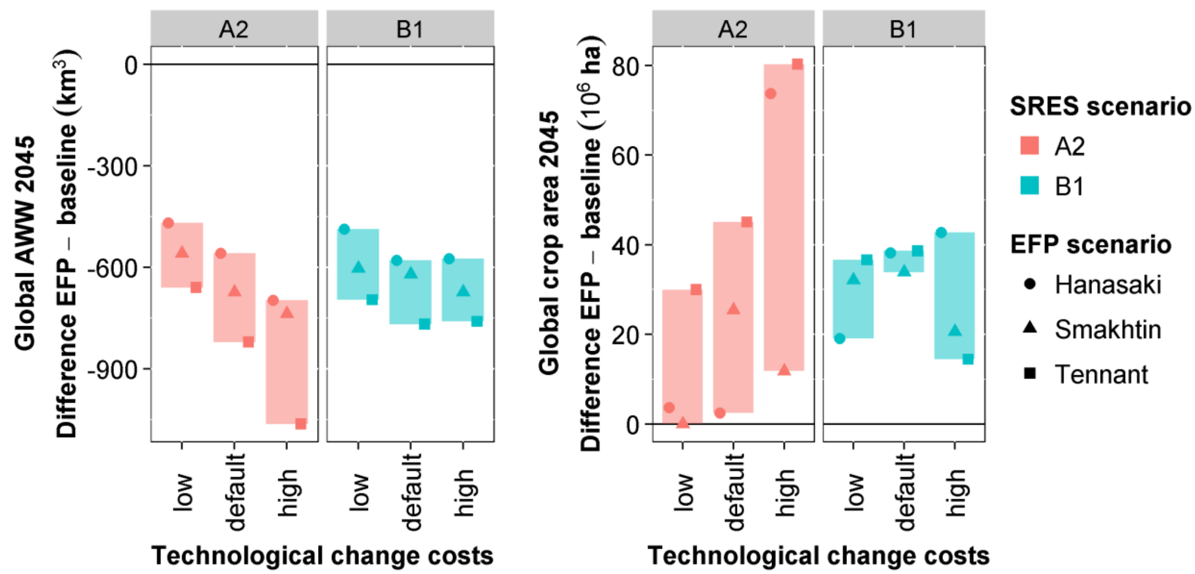

Figure D1 Changes in global agricultural water withdrawals (AWW, left) and crop area (right) due to EFP in 2045. Three different assumptions on the costs of yield increasing technological change (low, default, high) are differentiated on the x-axis. Colors differentiate socioeconomic scenarios. EFP scenarios are distinguished by the shape of points. Shaded areas span the full range of EFP impacts under the respective socioeconomic scenario.

D.2 Annual irrigation costs

We find that annual irrigation cost assumptions have little impact on the implications of EFP on global AWW (Figure D2, left). Higher costs can however lead to increased cropland expansion due to EFP under the A2 scenario, especially for the Hanasaki EFP scenario (107 Mha). The picture is different under the B1 scenario, where higher costs as well as lower costs lead to decreased cropland expansion due to EFP (below 30 Mha in 2045).

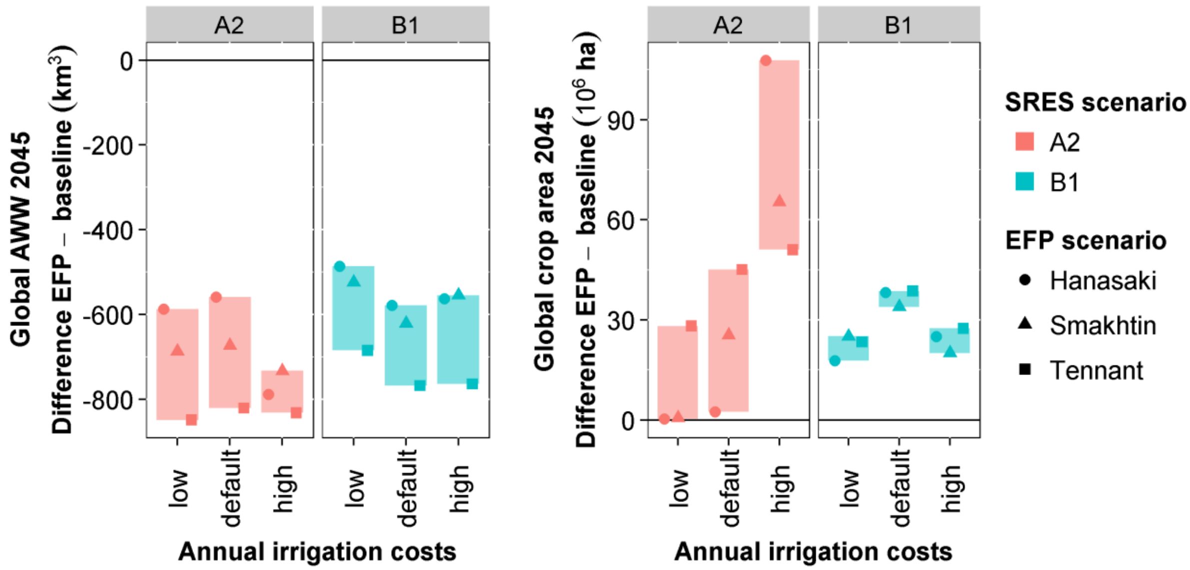

Figure D2 Changes in global agricultural water withdrawals (AWW, left) and crop area (right) due to EFP in 2045. Three different assumptions on the annual operation and maintenance costs irrigation systems (low, default, high) are differentiated on the x-axis. Colors differentiate socioeconomic scenarios. EFP scenarios are distinguished by the shape of points. Shaded areas span the full range of EFP impacts under the respective socioeconomic scenario.

D.3 Investment costs for irrigation infrastructure

The implications of EFP for AWW are not very sensitive to changes in irrigation investment costs (Figure D3, left). Changes in cropland due to EFP show a stronger dependence on the EFP scenario for regional and global investment cost assumptions than for the default value, especially for the A2 scenario. With global irrigation investment costs, EFP can lead to a decrease in crop area by up to 90 Mha in 2045 for the Hanasaki scenario. The sensitivity of model results with respect to irrigation investment costs in B1 is less pronounced than in A2.

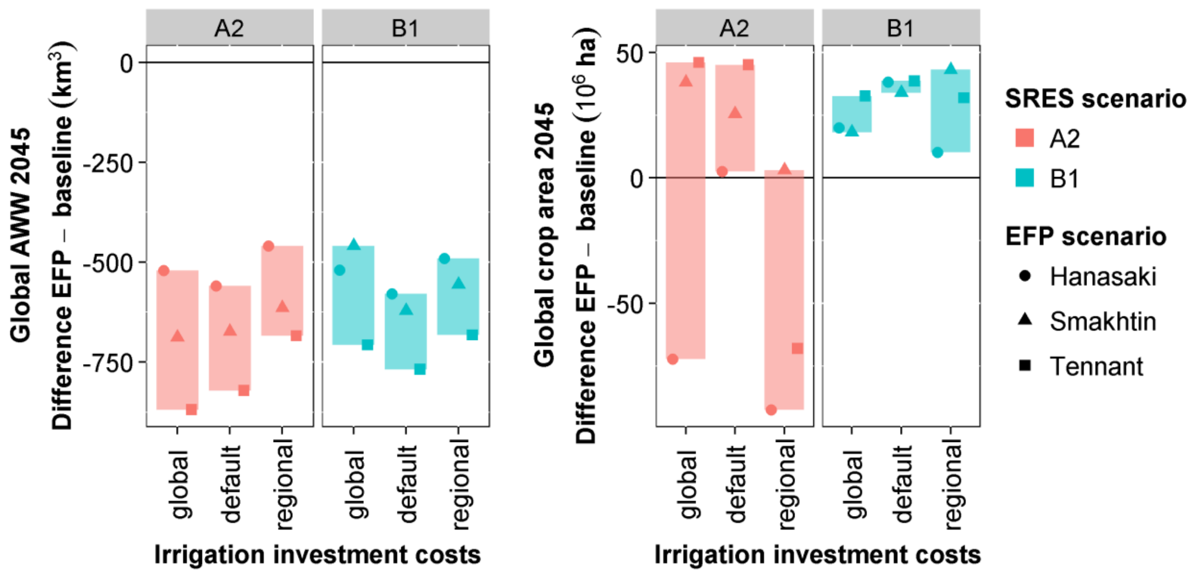

Figure D3 Changes in global agricultural water withdrawals (AWW, left) and crop area (right) due to EFP in 2045. Three different assumptions on investment costs for installing new irrigation systems (regional, default, global) are differentiated on the x-axis. Colors differentiate socioeconomic scenarios. EFP scenarios are distinguished by the shape of points. Shaded areas span the full range of EFP impacts under the respective socioeconomic scenario.